A Graphical Method for Estimating Charge
Collected by Diffusion from an Ion Track

Larry D. Edmonds
(818) 354-2778,   FAX (818) 393-4559

Jet Propulsion Laboratory
California Institute of Technology
Mail Stop 303-220
4800 Oak Grove Drive
Pasadena, California 91109-8099

ABSTRACT

  A graphical method is presented for the calculation of charge
collection by diffusion from an ion track in a silicon device.
Graphical data are provided for several device geometries. The
ion track location/orientation is arbitrary.

----

1. <u>Introduction</u>

A graphical method estimates collected charge, predicted by the linear diffusion equation, produced by an ion track in a simple silicon structure consisting of a uniformly doped substrate bounded by a collection of reflective (insulated) boundary surfaces and a collection of sinks for excess carriers. Each sink simulates some structure such as a reverse-biased depletion region (DR) boundary (DRB) or an ohmic contact (electrode) . Bulk recombination is neglected and all recombination is assumed to be on the sink boundaries. This is often an adequate approximation. When in doubt, the discussion in Section 4 may help (Auger recombination is briefly mentioned in Section 6). The theory can easily be generalized to include bulk recombination losses (as pointed out in Section 7), but the required graphical data are not provided here.

The linear diffusion equation has been used in the past to predict currents at DRB's produced by lightly ionizing particles such as alpha particles [1,2]. Heavier particles are able to collapse a DR to the extent that funneling [3,4] may become important. But even when funneling necessitates use of the nonlinear drift/diffusion equations, the solution still requires that we know how to estimate currents predicted by the linear diffusion equation (among other things) [5]. Therefore, this equation will often find applications in the analysis of ion-induced currents.

Several variations of this problem have been solved in the past. Wouters [1] and Kirkpatrick [2] have both treated the problem in which the upper substrate surface contains a sufficiently high density of DR's so that the entire upper surface can be approximated as a sink. Reference [6] treated the problem in which the upper surface contains one isolated DR. Only total collected charge was estimated in Reference [6]. No collection time was estimated, but it was still possible to include bulk recombination losses. However, the Reference [6] method has limitations. The lower substrate surface (electrode) must be far below the ion track and the track cannot be too close to the DR. The present analysis removes these restrictions, but a new limitation is that recombination in the substrate interior must have a negligible effect on the collected charge of interest. In theory, there are no restrictions on the substrate or track geometries (except that it be okay to neglect recombination in the

substrate interior) . In practice, charge collection estimates can be obtained for any substrate geometry such that equipotential surfaces (associated with **Laplace's** equation) have been plotted. Examples are in the appendix. Total (time integrated from zero to infinity) collected charge is rigorously quantified for arbitrary geometries. An estimate of the time duration of charge collection is derived for arbitrary geometries, but explicitly evaluated only for one-dimensional and spherical geometries. This estimate includes the influence of boundary surfaces. In one extreme case, boundary surfaces have little influence and the estimate reduces to the traditional estimate (the square of the **source-to-**destination distance, divided by the **diffusion** coefficient). In the opposite extreme, boundary surfaces have a strong influence, and charge collection is six times faster than indicated by the traditional estimate. Physical and statistical explanations are given.

2. Analysis

Figure 1 shows a simple geometry, consisting of one upper sink (representing a DRB) above a flat lower sink (representing an electrode) . More generally, the substrate is bounded by any collection of sinks which are separated by reflective surfaces. Let S_2 denote the surface that collected charge is to be calculated for. If we want to know the charge collected by a particular DRB, then S_2 is that DRB. If we want to know the sum of the charges collected by a set of **DRB's,** then S_2 is the union of that set of **DRB's.** Let S_1 be the union of all remaining sink boundaries. Let P denote the excess carrier density (assumed to be the same for minority and majority **carriers)** . The linear diffusion equation is assumed to apply, so P **is** governed by the boundary value problem

$$D \ div \ grad \ P = \delta P / \delta t \quad \text{in substrate} \tag{1a}$$

$$P = o \quad \text{on } \mathbf{S_1} \text{ and on } S_2 \tag{1b}$$

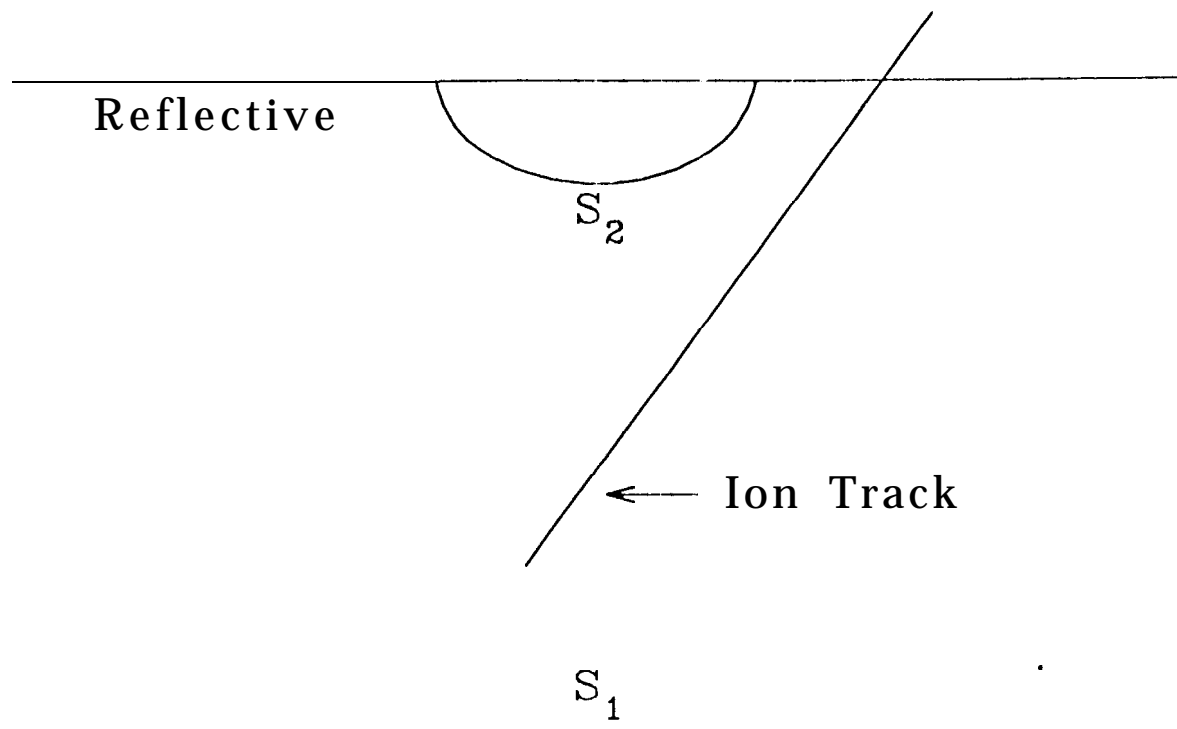$$P = \mathbf{P_I} \quad a \ t \ t = O \tag{1c}$$

3

Figure 1: A simple geometry. A single sink S_2 (possibly a DRB) is above an infinite plane sink S_1 (an ohmic contact) .

where $\delta/\delta t$ denotes partial derivative with respect to time and P_I is the density of electron-hole (e-h) pairs liberated by the ion. The diffusion coefficient D is assumed to be a constant. Reflective boundary conditions are assumed on the reflective boundaries. The diffusion current at S_2 is denoted I(t) and defined by

$$I(t) \equiv - q D \int_{S_2} grad \ P \ .ds \qquad (2)$$

where q is the elementary charge. The unit normal vector in the surface integral is directed outward from the substrate, so that I(t) is positive. The collected charge at S_2 is denoted Q and defined by

$$Q \equiv \int_0^\infty I(t) \ dt. \ . \qquad (3)$$

Q can be calculated without explicitly solving for P, but it is necessary to solve for the potential Ω, which is the solution to Laplace's equation satisfying

$$div \ grad \ \Omega = O \quad in \ substrate \qquad (4a)$$

$$1=1o \quad on \ S_1 \quad and \ \Omega = 1 \quad on \ S_2 \qquad (4b)$$

with reflective boundary conditions assumed on the reflective boundaries. The potential Ω, which has nothing to do with carrier density, is created in the physically unrelated problem in which the substrate satisfies Ohm's law with a uniform conductivity and a unit potential is applied to S_2 with S_1 grounded. Because Ω does not depend on the initial carrier density, it only has to be solved once for each geometry. The same Ω is used to calculate Q for all ion tracks. To see how this is done, use (1), (2), (4), and the divergence theorem to get

$$-I(t)/(q\,D) = \int \Omega\ \mathbf{grad}\ \mathbf{P} \cdot \mathbf{ds} - \int P\ grad\ \Omega \cdot ds$$

$$= \int_I n\ div\ grad\ \mathbf{P}\ d3x = (1/D) \int n\ \delta\mathbf{P}/\delta\mathbf{t}\ d3x \qquad (5)$$

where surface integrals without. subscripts are over the closed boundary, and the volume integrals are over the substrate. Integrating in t gives

$$Q = q \int n\ PI\ d3x\ . \qquad (6)$$

The integral in (6) can be evaluated numerically. Select a number M. Then select a set of numbers vi satisfying $0 = v_0 < v_1 < \ldots < v_M = 1$. For each i=1, ... M, define the region Ri by

$`_i \equiv$ the region between the $\Omega = vi_{-1}$ **equipotential** surface and the $\Omega = \mathbf{v_i}$ equipotential surface.

The integral in (6) can be written as

$$Q = q \sum_{i=1}^{M} \int_{R_i} \Omega\ P_I\ d^3x \approx q \sum_{i=1}^{M} [(vi + v_{i-1})/2] \int_{R_i} P_I\ d^3x$$

where the approximation on the far right can be made as accurate as we want by using a sufficiently fine partition. For each i=1, ... M, define ni by

$`_i \equiv$ number of e-h pairs initially liberated between the $n = `_{i-1}$ surface and the $\Omega = \mathbf{v_i}$ surface. $\qquad (7)$

The equation for Q becomes

$$Q \approx q \sum_{i=1}^{M} [(v_i + v_{i-1})/2] \, n_i. \tag{8}$$

With an initial track density PI given, all that is needed to calculate Q is a plot of the Ω equipotential surfaces so that each n_i can be calculated from (7).

3. Discussion of the Figures and an Example

Collected charge can be calculated from (7) and (8) if we have figures showing constant Ω surfaces. Some figures are provided in the appendix for the case in which the sink of interest S_2 is a flat circular disk. The figures can also be used to represent other "unflat" circular shapes, but this is discussed later. For the time being, S_2 is imagined to be a flat disk of diameter DI. Several variations of this geometry, characterized by the presence or absence of other structures, are discussed below.

The simplest geometry is that in which S_2 is very far from all other structures. It lies in a horizontal reflective plane and S_1 is at infinity, below an infinitely thick substrate. Constant Ω surfaces are well known for this geometry and are represented by contours in Figure Al (appendix) . The axis of symmetry is in the plane of the page and double lines represent reflective boundaries. All contours intersect the reflective boundary at right angles, but limited plotting resolution does not make this visible in the figure. The inset "DI=4 min. div." means that the disk diameter is four minor divisions, which can represent any physical distance. Contour labels are the Ω values. The 1.0 contour is S_2 " Contours outside of the 0.1 contour are nearly circular. If desired, the plot can be extended to greater distances by drawing circles and assigning Ω values from the equation $\Omega \approx (1/\pi)(DI/r)$, where the radial distance r is measured in the same units that DI is measured in.

An ion track is not shown in the figure because it is supplied by the user. This simple geometry cannot be used if the track is

too long, even if DI is much smaller than all other relevant dimensions. Other relevant dimensions, denoted collectively as OD , are diffusion length, substrate thickness, and distance between S_2 and other structures in the horizontal plane (e.g., other DRB's) . As track length increases without bound, predicted collected charge also increases without bound, becoming singular as the logarithm of the track length. At least one of the OD must be recognized as finite, and a different figure is needed (discussed below) .

A common situation in which the simplest geometry is inappropriate occurs when S_2 is a member of an array of DRB's, with the array dense enough to influence charge collection at S_2. The union of all DRB's, except S_2, is S_1. The potential Ω is derived from the electrostatics problem in which one disk, S_2, is at unit potential and is surrounded by a dense array of grounded structures. Let SP be the nearest neighbor spacing, measured from closest point to closest point. The grounded array will screen most of the potential produced by S_2 if the observation Point is in the horizontal plane and more than a distance SP from S_2. The grounded array is simulated by grounding the entire section of the horizontal plane where r>(1/2)DI+SP, with the radial coordinate r measured from the center of S_2. The surface S_1 now becomes this planer section. The simplified boundary conditions governing Ω now become $\Omega=1$ on the planer section where r<(1/2)DI (which is S_2), $\Omega=0$ on the planer section where r>(1/2)DI+SP (which is S_1), and with reflective boundary conditions on the planer section between S_2 and S_1. We will pretend that this is the original problem that was to be solved, so that we do not have to call this an approximation. But even this problem will only be approximately solved.

An approximate solution is obtained by starting with the potential function for an isolated disk and then using the method of inversion [7] to construct a second solution to Laplace's equation. An appropriate superposition of these two solutions, denoted Ω, will approximately satisfy the required boundary conditions. Note that Ω is the exact solution for some geometry, although not the intended geometry. By tracing equipotential surfaces to find out where $\Omega=1$ and where $\Omega=0$, we determine the geometry that Ω exactly fits. The 1.0 surface in any figure in the appendix is the actual S_2, i.e., the surface where Ω really is 1, as opposed to the surface where Ω was intended to be 1. Similarly for S_1. Figures A2, A3, and A4 show Ω contours con-

strutted by this method for several values of the ratio SP/DI. Because the intended boundary conditions are not exactly satisfied, S_2 and S_1 are not perfectly flat, but they are flat enough (especially S_2).

   Figures A2, A3, and A4 have different parts (e.g. , an "a" and "b" part for Figure A2) showing different levels of magnification. In each case, the last contour plotted resembles that for an electric dipole, so that simple analytical fits can be used to extend the plots beyond the ranges shown. For example, at loca⁻ tions outside of the O.O2 contour in Figure A2, the extension is given by $\Omega \approx 0.02(z_c/r)^2 \cos\phi$, where r and ϕ are the obvious coordinates and z_c is the distance on the axis of symmetry from S_2 to the 0.02 contour, measured in the same units that r is measured in. Similar extensions apply to Figures A3 and A4.

   Another interesting geometry is the same as that just considered, except that the "substrate" is an epi layer. There is now a reflective plane some distance L below the plane that S_2 and S_1 lie in. Another approximation is used to obtain Ω. By starting with the Ω derived for the previous problem and adding an appropriate translation (or image) of the same function, reflective boundary conditions will be satisfied on the lower plane. An appropriate series of translated functions will satisfy all required reflective boundary conditions, but boundary **values** at the locations where S_2 and S_1 are intended to be are disturbed. Suitably chosen multiplicative and additive constants help a little, and produce the Ω used for this problem. As before, Ω is the exact solution for some geometry, although not the intended geometry. Figures A5 through **A10** show Ω contours constructed by this method for several values of **SP/DI** and **L/DI.** Because the intended boundary conditions are not exactly satisfied, S_1 is not very flat. The most extreme cases, shown in the figures, of an **"unflat"** S_1 are in Figures A9 and A1O. But even if S_1 was the planer section that it was supposed to be, the potential would still be rapidly attenuated as the observation point moves under S_1. It should not make much difference how flat S_1 is in these extreme cases. In general, the **SP/DI** and L/DI ratios such that S_1 deviates most from its intended shape are also the ratios such that the shape of S_1 is least important. Only one level of magnification is shown for Figures A5 through A1O. The high density of contours will cause the figures to **be** too crowded if all contours are labeled. The pattern of contour values is consistent, and reminders are included in the figure captions.

The figures offer additional flexibility by renormalizing the **equipotential** surfaces. DRBs are not really flat and if we do not want to approximate a given DRB as being flat, then it will not fit any of the sinks in the figures. But it might fit the 0.5 surface (for example) in one of the figures. By **renormalizing,** the 0.5 surface becomes the 1.0 surface (S_2), while the 0.4 surface becomes the 0.8 surface, etc. Another possible motivation for renormalizing is to obtain **SP/DI** ratios other than those listed in the figures. By **renormalizing,** a few figures can be made to represent a lot of different geometries.

Calculation of Q is especially convenient if the ion track has a uniform linear density and can be sketched into one of the figures. This can only be done if the track is in some plane containing the axis of symmetry. The most versatile approach for any other conditions is to approximate the track as a superposition of discrete points and treat each point individually. An example may help to clarify the calculation, and is shown in Figure 2. This is the same as Figure A1 except that a physical dimension (a 4 μm disc diameter) was assigned, and a track was sketched into the figure. For simplicity, the track lies in the plane of the page so that it can be sketched into the figure. The sink of interest is a flat disk, so **renormalizing** is unnecessary. The track conveniently ends at the 0.1 contour. If the track was longer, we could extend the plot by drawing some circles. The track has a uniform linear density of 6.47x104/pm, corresponding to a linear energy transfer (LET) of 1 **MeV-cm^2/mg** in silicon (assuming that each 3.6 **eV** of deposited energy liberates one electron-hole pair) . If we want the LET to be 40 instead of 1, we simply multiply the calculated value of Q by 40. By using the tick marks in the figure to make a paper ruler and literally measuring line segments in the figure, we find that about 2.8 μm of track is between the $\Omega=0.4$ and the $\Omega=0.5$ **equipotential** surfaces. The number of initial minority carriers (or e-h pairs) between these surfaces is about 1.8x105. We multiply this number by the average contour value, which is 0.45, to obtain one of the terms in (8), i.e., about 45% of this group of carriers will reach S_2. The same procedure is applied to the other track sections and the terms are added. The result is
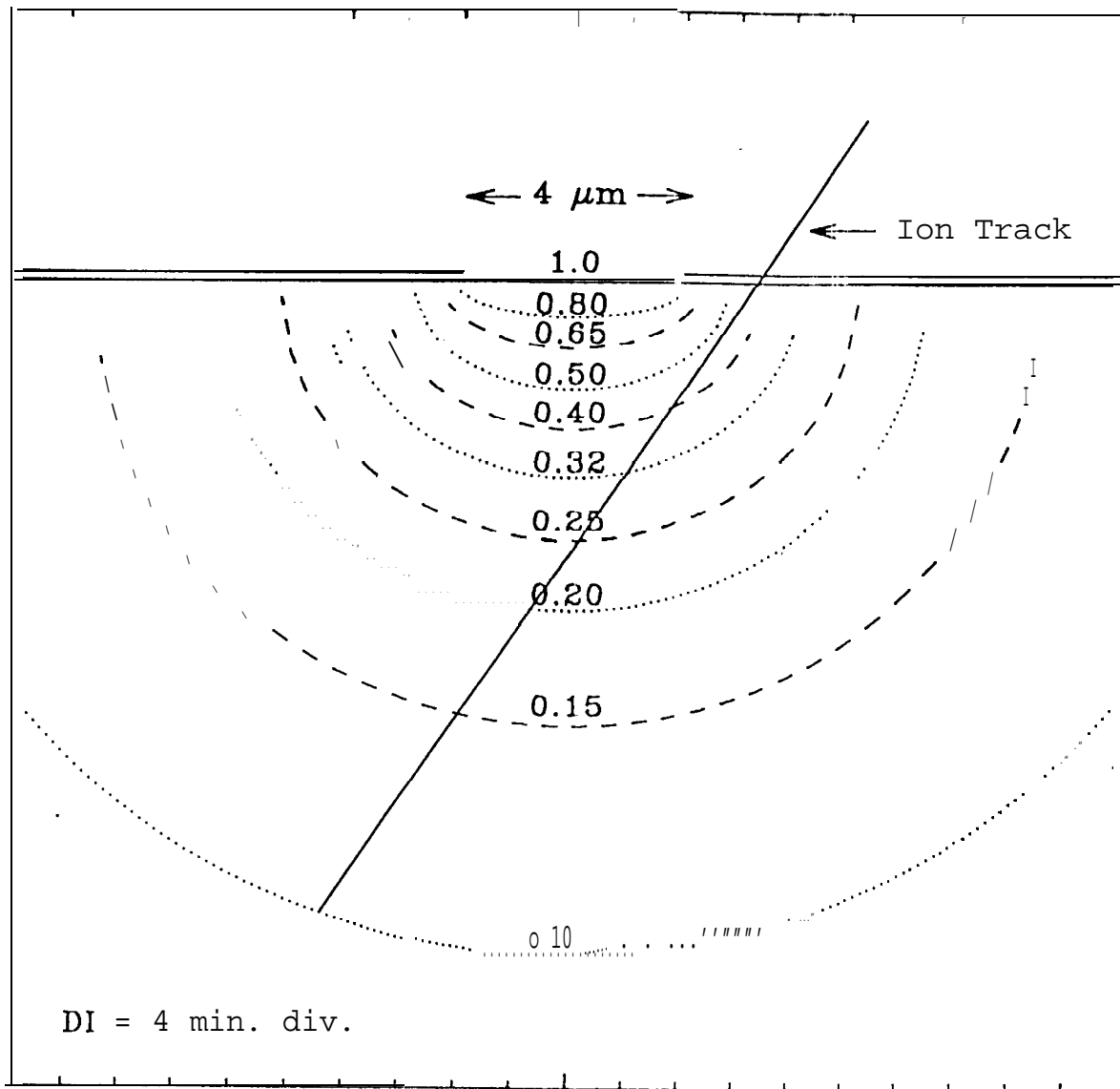
Figure 2: An example used to illustrate how Q can be calculated.

$$Q \approx q \, [\, (0.45)(1.8x105) + (0.36) \, (9.1x10^4) + (0.285) \, (1.0x105)$$

$$+ (0.225) \, (1.0x105) + (0.175) \, (1.5x105) + (0.125) \, (3.0x105)]$$

$$\approx 3.7X10\text{-}1^4 \, \text{coul.}$$

4. **Assessing** the Importance of Recombination

It is not always obvious whether or not **it** is okay to neglect recombination, because the importance of recombination can depend on which sink charge collection is to be calculated for. Even if many carriers recombine, charge collection at S_2 will not be strongly effected by recombination if few of these lost carriers would have reached S_2 anyway **(i.e., if** they would have gone to S_1 instead) . Recombination can be neglected if most charge collection at S_2 is from carriers initially close to S_2, compared to the diffusion length. Whether or not this condition is satisfied can be determined by first calculating Q with recombination neglected, as was done in the example in the previous section. Then determine what fraction **of** Q came from carriers initially within some fraction (let us say 1/2 to be definite) of a diffusion length from S_2. If this fraction of Q is nearly all of Q, it is okay to neglect recombination. Otherwise, we have a problem. A solution, pointed out in Section 7, is to construct more figures, but such figures are not provided here.

5. **Average** Arrival Time

The objective of this section is to get an order of magnitude estimate of the time duration of charge collection at S_2. Each carrier group in (7) contributes additively to the current, so we can get a picture of the time dependence of charge collection from the combined groups if we start with a picture of the time dependence of collected charge for each individual group. It is therefore sufficiently general to consider a single group, i.e., to assume that all carriers are initially liberated close to some point $\mathbf{x_S}$, which will be called the source coordinate. A statistical average arrival time (time of arrival at S_2) , associated with carriers initially near $\mathbf{x_S}$, will provide a measure of how fast or

slow charge collection from **this** group of carriers is. Average arrival time will first be defined as it is defined in statistics. Then an equation will be derived that solves for this arrival time (in theory) . The equation will then be explicitly solved, but only for one-dimensional and spherical geometries. The simple geometries provide a simple illustration of some interesting statistical and physical concepts regarding the influence of boundary surfaces. Quantitative results derived for simple geometries may provide order of magnitude estimates for some other geometries if we can estimate "effective distances", intended to make an irregular geometry conform to a simple geometry. Although the analysis eventually specializes to simple geometries, it begins by treating arbitrary geometries. The motivation for starting with a general treatment is that one of the equations to follow looks nice, even when it cannot be solved analytically. Furthermore, this "nice-looking" equation can be solved numerically, and provides opportunities for future developments.

In order to define average arrival time as it is defined in statistics, we need to find statistical interpretations for some of the physical quantities. **By** assumption, all carriers are initially near the source coordinate, so PI is given by

$$Pi(x) = n \; \delta(\mathbf{x} - \mathbf{x_S}) \tag{lo}$$

where n is the total number of e-h pairs liberated and δ is the **Dirac** delta function. Q is calculated from (6) with the result

$$Q = q \, n \, \Omega(\mathbf{x_S}) \; .$$

The total number of liberated minority carriers is n, while the total number that eventually reach S_2 (instead of $\mathbf{S_1}$) is Q/q. The fraction of carriers that eventually reach S_2 is $\Omega(\mathbf{x_S})$, so

$\Omega(\mathbf{x_S})$ = probability of a carrier, initially near X_S, eventually reaching S_2.

The current $I(t)$ produced by the n carriers is related to a probability density or distribution. For some small time interval δt, the number of carriers that reach S_2 between time t and time $t+\delta t$ is $(1/q)I(t)\delta t$. The fraction of carriers that arrive at S_2 during this time interval is $(1/q)I(t)\delta t/n$, so

$$(1/q) \, [I(t)/n] \, \delta t = \text{probability for arrival at } S_2$$
$$\text{between times t and } t+\delta t.$$

Now consider the subset of carriers that eventually reach S_2. The number of such carriers is $n\Omega(x_S)$. The fraction of these carriers that reach S_2 between times t and $t+\delta t$ is $I(t)\delta t/[qn\Omega(x_S)]$. Therefore a conditional probability density is

$$I(t)/[q \, n \, \Omega(x_S)] = \text{probability density for the arrival} \qquad (11)$$
$$\text{time at } S_2 \text{ to be t, given that } S_2$$
$$\text{is eventually reached.}$$

The average arrival time is denoted T and defined to be the integral of t multiplied by the probability density for the arrival time to be t. Using (11), the definition becomes

$$T \equiv [q \, n \, \Omega(x_S)]^{-1} \int_0^{\infty} t \, I(t) \, dt \, . \qquad (12)$$

Having defined T, the next step is to find a way to solve it, without literally solving the time dependent diffusion equation to solve for $I(t)$. This can be done by integrating (la) with respect to t, from 0 to ∞, while using (10) to conclude that the time integral of P satisfies Poisson's equation with a delta function driving term. Therefore

$$\int_0^{\infty} P(x,t) \, dt = (n/D) \, G(x,x_S) \qquad (13)$$

where the Greens function G is defined by

$$\text{div grad } G(\mathbf{x}, \mathbf{x}_S) = - \delta(\mathbf{x} \bar{} \mathbf{x}_S) \quad \text{in substrate} \tag{14a}$$

$$G(\mathbf{x}, \mathbf{x}_S) = 0 \quad \text{if x is on } S_1 \text{ or on S2} \tag{14b}$$

with reflective boundary conditions assumed on the reflective boundaries. Multiplying (5) by t and integrating and then using an integration by parts on the right gives

$$\int_0^\infty t\ I(t)\ dt = q \int \Omega \int_0^\infty P\ dt\ d3x$$

and (13) gives

$$\int_0^\infty t\ I(t)\ dt = q\ (n/D) \int \Omega\ G(\mathbf{x}, \mathbf{x}_S)\ d3x\ . \tag{15}$$

The integral containing the Greens function can be expressed another way by defining the function U by the boundary value problem

$$\textbf{div grad } U(x) = - \Omega(\mathbf{x}) \quad \text{in substrate} \tag{16a}$$

$$u(x) \bar{} o \quad \text{if } \mathbf{x} \text{ is on } S_1 \text{ or on } S_2 \tag{16b}$$

with reflective boundary conditions assumed on the reflective boundaries. A familiar application of the divergence theorem using (14) and (16) will show that the integral on the right side of (15) is $U(\mathbf{x}_S)$. Substituting this result into (12) gives

$$T(\mathbf{x}_S) = (1/D)\ U(\mathbf{x}_S)/\Omega(\mathbf{x}_S) \tag{17}$$

13

where the argument x_S is now included to emphasize the fact that T depends on the source coordinate.

Equation (17) is a special form of the nice-looking equation that was promised (a difficulty discussed below necessitates a more general form that will be derived later) . This equation shows that T can be calculated by solving Poissonts equation (16) for U. This equation requires numerical **methods** for most geometries, but is easy to solve for one-dimensional and spherical geometries.

First consider the one-dimensional problem. Let L be the distance between S_1 and S_2 (not to be confused with the L in Figures A5 through A10), and let x be measured from S_2 so that x_S is the distance between the source point and S_2. The potential Ω is given by

$$l-l(x) \; \bar{} \; 1 - x/L$$

and the solution to (16) is

$$u(x) = (L^2/6) \, [(1. - x/L) - (1 - x/L)^3]$$

so that (17) becomes

$$T(x_S) = L \, x_S/(3D) - x_S^2/(6D) \quad \text{(one-dimensional)} \quad . \quad (18)$$

Now consider the spherical problem in which S_1 and S_2 are concentric hemispheres below a horizontal reflective plane. Let r_i be the radius of S_i (i=1,2) and assume that $r_1 > r_2$. Let r be the radial coordinate of an arbitrary point so that

$$\Omega = [r_1 \, r_2/(r_1 - r_2)] \, [1/r - 1/r_1]$$

and the solution to (16) is

$$U(r) = (1/6) [r_2/(r_1 - r_2)] [(r - r_1)(r - 2r_1)$$

$$+ r_2 (2r_1 - r_2)(1 - r_1/r)]$$

and (17) becomes

$$T(r_s) = [(r_2 - r_1)^2 - (r_s - r_1)^2]/(6D) .$$

If we let $x_s \equiv r_s - r_2$ be the distance from source to S_2, and $L \equiv r_1 - r_2$ be the distance from S_2 to S_1, the equation becomes

$$T(x_s) = L \, x_s/(3D) - x_s^2/(6D) \qquad \text{(spherical)} . \qquad (19)$$

Note that we could have started with the slightly more complicated spherical problem and then derive the one-dimensional result by letting r, r_1, and r_2 go to infinity in such a way that L and x_s are constant.

It is interesting that the average arrival time depends not only on the source to destination distance x_s, but also on L. The fact that T depends on other geometric parameters in addition to x_s could have been anticipated on a macroscopic level by thinking of the heat equation, which is the same diffusion equation that we are treating. The source coordinate is an initial hot spot while the sinks are cold contacts. The collection time for heat flux through S_2 is correlated to how fast the device is cooling off, because the heat flux at any point dies out fast if the device cools off fast. The rate of device cooling is strongly influenced by device geometry, so the time duration of heat flow through S_2 depends on geometry. If we decrease L in (19) (the smallest allowed value is x_s) , we find that T decreases because the device cools off faster. From a microscopic point of view (and considering carriers again instead of heat), the location of S_1 affects the carrier population that defines the statistics. Carriers that reach S_1 are eliminated and do not contribute to the average arrival time at S_2. If S_1 is close to the source

coordinate, the carriers that reach S_2 take a relatively direct route (their random walks do not zig-zag back and fourth across S_1) and the average arrival time is relatively short.

Equation (19) has an unfortunate property if we let $L \to \infty$. The average arrival time increases without bound, even if x_S is fixed when taking this limit. The physical explanation is that a small fraction of carriers arrive very late. The arrival time is large enough to more than compensate for the smallness of this fraction of carriers, in the sense that this negligible fraction is strongly influencing the average arrival time. The statistical explanation is that the distribution (11) is so skewed (it decreases so slowly with increasing t) that it does not have a mean. If L is finite (so that T is finite) but very large (so that T is unphysical), then T has a precise statistical meaning but no physical meaning.

The carriers that arrive very late are so few in number that they have little physical significance, and their only effect is to make average arrival time physically meaningless when L is large. One way out of this problem is to simply ignore some of the late arrivals. For example, we might ignore the last 10% of the carriers when estimating average arrival **time. One obvious** objection to this approach is that the selected fraction is arbitrary. (Why 10% instead of 5%?) But we are going to have to be willing to accept some arbitrariness. Even if the time dependent diffusion equation was completely solved and collected charge was plotted as a function of time, some ad hoc criterion is still needed in order to obtain a single number that represents charge collection time. Given that some arbitrariness is unavoidable, the primary problem with selecting some fraction is that the resulting average arrival time is too difficult to calculate, unless we completely solve the equations. Another approach that produces a similar end result, but leads to a simpler analysis, is to include an artificial recombination term in the diffusion equation. Recombination automatically eliminates most carriers that would otherwise arrive very late. Using an appropriately selected lifetime τ, we can obtain an end result that is similar to neglecting the last such-and-such fraction of carriers when computing average arrival time.

Selection of a value for τ is postponed until later. For the time being, τ is an arbitrary constant. Average arrival time T_τ, associated with τ, is defined by first modifying (1) so that it

becomes

$$D \ \text{div grad} \ \mathbf{P}_\tau = (1/\tau + \delta/\delta t) \ \mathbf{P}_\tau \qquad \text{in substrate} \qquad (20a)$$

$$\mathbf{P}_\tau = 0 \qquad \text{on } S_1 \text{ and on } S_2 \qquad \qquad (20b)$$

$$\mathbf{P}_\tau = \mathbf{P}_I = n \ \delta(\mathbf{x} - \mathbf{x}_s) \qquad \text{at } t = 0 \ . \qquad (20c)$$

The current and collected charge are defined by

$$I_\tau(t) \equiv - q \ D \int_{IS_2} \text{grad} \ \ \mathbf{P}_\tau \cdot \mathbf{ds} \qquad (21)$$

$$Q_\tau = \int_0^{00} I_\tau(t) \ dt \ . \qquad (22)$$

The average arrival time is defined by

$$T_\tau \equiv (1/Q_\tau) \ \Big|_0^\infty t \ I_\tau(t) \ dt \ . \qquad (23)$$

The denominator in (23) is the total number of carriers (times q) that eventually reach S_2, so $\mathbf{T}_\tau$ is derived from a conditional probability density similar to (11). Therefore, $\mathbf{T}_\tau$ has a precise statistical interpretation as a mean arrival time. But this mean refers to a population of carriers that are subject to recombination, which eliminates most of the carriers that would otherwise arrive very late (and a few that would otherwise arrive early).

The quantities P, I, and Q without the τ subscript are defined by the infinite lifetime equations in Section 2. It is easy to show that the solution to (20) is

17

$$P_\tau = e-t/T \, P$$

so that (21) gives

$$I_\tau(t) = e^{\cdot}t/T \, I(t) \; . \tag{24}$$

Regarding IT(t) as a function of 7, differentiating (24) gives

$$\delta I_\tau(t)/\delta(1/\tau) = - \, t \, e^{-t/\tau} \, I(t) = - \, t \, I_\tau(t)$$

so that (23) becomes

$$T_\tau = - \, (1/Q_\tau)\delta Q_\tau/\delta(1/\tau) \quad . \tag{25}$$

We can solve for Q_τ by first defining Ω_τ by the boundary value problem

$$D \; div \; grad \; \Omega_\tau = (1/T) \, \Omega_\tau \quad in \; substrate \tag{26a}$$

$$\Omega_\tau = 0 \quad on \; S_1 \quad and \; \Omega_\tau = 1 \quad on \; S_2 \; . \tag{26b}$$

A familiar application of the divergence **theorem** using (20) and (26) gives

$$- \, (1/q) \, I_\tau(t) = D \int_{S_2} grad \quad P_\tau . ds = \int_I \Omega_\tau \, \delta P_\tau/\delta t \; d3x$$

so (22) becomes

$$Q_\tau = q \int \Omega_\tau \, P_I \; d3x = q \, n \int \Omega_\tau \, \delta(x - x_S) \; d3x$$

or

$$Q_\tau = q^n \Omega_\tau(\mathbf{x}_s) \qquad (27)$$

and (25) becomes

$$T_\tau(\mathbf{x}_s) = - [1/\Omega_\tau(\mathbf{x}_s)] \, \delta\Omega_\tau(\mathbf{x}_s)/\delta(1/\tau) \; . \qquad (28)$$

Equation (28) is the general form of the nice-looking equation that was promised. Although incidental to this discussion, it is interesting that higher statistical moments (e.g., variance) can be derived in a similar way, with the result expressed in terms of higher $1/\tau$ derivatives. Equation (28) can be made to look more like the special case (17) if we define U_τ by

$$UT(X) \equiv - D \, \delta\Omega_\tau(\mathbf{x})/\delta(1/\tau) \qquad (29)$$

By differentiating (26) with respect to $1/T$, we conclude that U_τ can also be calculated from the boundary value problem

$$D \operatorname{div} \operatorname{grad} U_\tau - (1/\tau) U_\tau = - D \, \Omega_\tau \qquad \text{in substrate} \qquad (30a)$$

$$U_\tau = 0 \qquad \text{on } S_1 \text{ and } \textbf{\textit{on }} S_2 \qquad \textbf{(30b)}$$

which is the generalization of (16). The equation for T_τ finally becomes

$$T_\tau(\mathbf{x}_s) = (1/D) \, U_\tau(\mathbf{x}_s)/\Omega_\tau(\mathbf{x}_s) \; . \qquad (31)$$

To solve for the average arrival time, we have the option of solving U_τ from the boundary value problem (30), or by taking the $1/\tau$ derivative in (29).

An explicit solution will now be derived for the same spherical problem that (19) applies to. As before, we let $L=r_1-r_2$ be the distance from S_1 to S_2, and $xs=rs-r_2$ be the distance between the source coordinate and S_2. An additional relevant length is the diffusion length L_D defined by

$$L_D \equiv (D \ \tau)^{1/2} \ . \tag{32}$$

The solution to (26) is given by

$$\Omega_\tau = (r_2/r) \ [\sinh(L/L_D)]^{-1} \ \sinh(r_1/L_D \ \bar{} \ r/L_D) \ . \tag{33}$$

We can use (29) to solve for U_τ. It is convenient to use (32) and the chain rule to express the derivative in (29) as

$$\delta/\delta(1/\tau) = (1/2)(L_D/D) \ \delta/\delta(1/L_D)$$

and using (33) gives

$$UT = (L_D/2) \ \Omega_\tau \ [L \ \coth(L/L_D) \ \bar{} \ (r_1 \ \bar{} \ r) \ \coth(r_1/L_D \ \bar{} \ r/L_D)]$$

so that (31) gives

$$T_\tau \ (x_S) \ \bar{=} \ (1/2)(L_D{}^2/D) \ [\ (L/LD) \ \coth(L/L_D)$$

$$- \ (L/L_D \ - \ x_S/L_D) \ \coth(L/L_D \ \bar{} \ x_S/L_D) \ ]. \tag{34}$$

By taking the limit as r_1, r_2, and rs become infinite with L and x_S fixed, we conclude that (34) also applies to the **one-dimensional** problem.

Note that if we first use (27) to solve for Q_τ as a function of τ, we can then use Laplace transforms with (22) and (24) to solve for I as a function of t. But the objective here is simpler. We

are looking for a single number that estimates the time duration
of charge collection at S_2, and is obtained by selecting a defi-
nite τ to be used in the average arrival time given by (34).
Recombination was artificially included to eliminate the small
population of carriers that would otherwise arrive very late and
strongly influence the average arrival time. A good value for τ
is a value such that most carriers heading towards S_2 do not
recombine, while most of the small population that would other-
wise arrive very late do. This suggests that τ should be selected
so that the diffusion length is several times the distance from
source to destination. The charge collection time T_c is defined
to be T_τ when τ is selected so that $L_D = 2x_S$. The **result** is

$$T_C(x_S) = (2x_S^2/D) [(L/2x_S) \coth(L/2x_S)$$

$$- (L/2x_S - 1/2) \coth(L/2x_S - 1/2)] . \qquad (35)$$

Two limiting cases are interesting. We first consider the large
L limit. When taking this limit, it is helpful to note that the
two hyperbolic functions approach each other (and approach 1)
faster than L increases, so that the L's in the square brackets
subtract out. The result is

$$T_C \rightarrow (2x_S^2/D) [1/2] = x_S^2/D \qquad \text{as } L \rightarrow 00 . \qquad (36)$$

The right side of (36) is a traditional estimate of the charge
collection time. In the opposite extreme, we let L approach its
smallest allowed value, which is x_S. This limit also applies if
we regard L as fixed and move the source coordinate towards S_1.
The result is

$$T_C \rightarrow (2x_S^2/D) [(1/2) \coth(1/2) - 1] \approx x_S^2/6D \qquad \text{as } L \rightarrow x_S . \qquad (37)$$

Comparing (37) to the same limit applied to (19), we find that
the artificial recombination has little effect on the average
arrival time in this limit, indicating that the few late arrivals
do not strongly influence average arrival time in this limit.
Note that charge **collection is six times faster, in this limit,**

than indicated by the more traditional estimate x_s^2/D. This is due to the influence of boundary surfaces. In the analogous heat problem discussed earlier, we can say that the rapid device cooling induced by the cold contacts shortens the time duration of heat flow to S_2.

6. Nonlinear Effects

Diffusion may adequately describe charge collection in some devices (e.g., DRAMs [8]) even when the ion LET is so large that the carrier density exceeds the doping density over an extended spatial region and time interval. The **ambipolar** diffusion equation is most likely to be used in this case, i.e., the D in (la) is the **ambipolar** diffusion coefficient. Some investigators will insist that neglecting carrier-carrier scattering **(CCS)** is a big mistake. The purpose of this discussion is to point out that including **CCS** is a bigger mistake, if it is not treated consistently. CCS affects carrier mobility, but a **consistent** treatment recognizes that CCS also modifies the Einstein relation used to calculate diffusion coefficients from nobilities. A theoretical analysis [9] has shown that the end result is that the **ambipolar** diffusion coefficient is not affected by CCS. This result can be intuitively guessed if we visualize **ambipolar** diffusion as a process in which electrons and holes move together in an average sense (in reality, electrons and holes do not always move together during **ambipolar** diffusion [5,10], but they do in some special cases and that is good enough for this discussion). We would not expect collisions between carriers to affect their average motions when both types of carriers have the same average motion. Failure to modify the Einstein relation can result in unphysical predictions, such as tracks being "frozen" for an extended time, as if the carriers were immobile until recombination reduces the population. This is mentioned because some computer simulation results have made such predictions. It is better to completely ignore CCS than to include it in one calculation but not in another. If CCS is treated consistently, we should get the same diffusion equation that we get by consistently neglecting CCS, which is the simplest approach.

All discussion in the previous sections regarding recombination in the substrate interior tacitly referred to **Shockley-Read-Hall**

22

recombination (SRHR) . Another type is Auger recombination (AR).
Although extremely nonlinear, AR may be easier to treat than SRHR
if certain required data are available. A theoretical analysis
[11] concludes that AR accompanying an expanding (diffusing)
track has such a short time duration that the end result is the
same as if there was no AR but the initial track density was
smaller, i.e., as if the ion had a reduced LET. For a given ion
species and energy combination **(ISEC)** , the "reduced LET" should
be a material property, dependent on AR lifetime but not on
geometry. This means that reduced LET is well defined, i.e., we
can associate a reduced LET with a given **ISEC in** a given material
just like we can associate a regular LET with a given **ISEC** in a
given material. Tabulation of reduced LET, derived from computer
simulations and/or measurements, may not be too formidable if AR
is important for a sufficiently narrow range of **ISEC's.** Further
discussion is beyond the scope of this paper. It is enough to
point out that a simple diffusion analysis, such as given here,
can probably include AR if the required data (reduced LET) are
available.

   Another nonl inear effect is "funneling", which occurs when
carriers flood a DR and cause it to collapse. Some or nearly **all**
of the applied voltage plus built-in potential normally across
the DR is now across the substrate. The substrate electric field
can enhance charge collection. A steady-state version of the
problem was solved fairly rigorously [5], and provided insights
into the transient problem that were confirmed by computer simu-
lations. But the analysis was quite complex, largely because the
potential drop (actual potential, not Ω) is divided between the
DR, the portion of substrate containing the track, and the por-
tion of substrate below the track. As transient charge collection
proceeds, the DR is *recovering* and the track length is shrinking
 (an important effect if the track **is** long enough to reach the
lower electrode) and the potential distribution becomes very com-
plex. A convincing transient **analysis** will probably not be much
simpler than the steady-state **analysis,** so it is not surprising
that the simple transient models that presently exist are too
simple. The transient problem has not yet been adequately solved
and it is not yet clear what role diffusion calculations will
play in the analysis. Diffusion can induce funneling under
steady-state conditions [5] and under transient conditions
[6,12], so it will clearly play some role in the transient prob-
lem. In the steady-state problem, diffusion calculations are not
enough but are still needed. Although not enough, having diffu-

sion current estimates for the transient problem must surely be better than not having them.

7. Recommendations for Future Work

The list of figures in the appendix is limited, and the use of simple analytic expressions limits the calculation of Ω to some rather special geometries. A more extensive set of figures obtained from modern numerical methods would be a useful contribution. Computer calculations can treat geometries that are better representations of some of the more common geometries found in actual devices. Three-dimensional geometries can be pictorially represented by plots in several planes, having the same orientations but translated relative to each other (the track can be approximated as a set of discrete points if it cannot be sketched into a figure). Recombination can also be included if the lifetime τ is approximated as a constant and (4) is replaced with (26). Although (26) is more difficult to solve analytically in three dimensions than (4), it is not a difficult equation if numerical methods are used. The primary disadvantage of (26) is that it introduces another parameter. **In addition to several** geometric dimensions, we now have another dimension; diffusion length. This means that a set of figures that could be called extensive would contain many pages. But they should be easy to make if the required computer codes are available.

REFERENCES

[1] s. Wouters, <u>Diffusion-Based Silicon Radiation Detectors,</u> Delft University Press, 1992.

[2] S. Kirkpatrick, "Modeling Diffusion and Collection of Charge from Ionizing Radiation in Silicon Devices," IEEE Transactions on Electron Devices, **vol.ED-26, no.11, pp.1742-1753,** November 1979.

[3] C. Hsieh, P. **Murley,** and R. O'Brien, "A Field-Funneling Effect on the Collection of Alpha-Particle-Generated Carriers in Silicon Devices," IEEE Electron Device Letters, **vol.EDL-2,** no.4, pp.103-105, April 1981.

[4] T. **Oldham,** F. McLean, and J. **Hartman,** "Revised **Funnel** Calcu‐ lations for Heavy Particles wit-h High **dE/dx,"** IEEE Transactions on Nuclear Science, **vol.33, no.6, pp.1646-1650,** December **1986.**

[5] L. Edmonds, <u>A Theoretical Analysis of Steady-State **Photocur-**</u> <u>rents in **Simple** Silicon Diodes,</u> Jet Propulsion Laboratory Publi‐ cation 95-10, March 1995.

[6] L. Edmonds, "Charge Collected by Diffusion from an Ion Track under Mixed Boundary Conditions," IEEE Transactions on Nuclear Science, **vol.38,** no.2, **pp.834-837, April 1991.**

[7] P. Morse and H. Feshbach, <u>Methods of Theoretical Physics,</u> McGraw-Hill, **p.1317,** 1953.

[8] J. Zoutendyk, L. Edmonds, and L. Smith, "Characterization of Multiple-Bit Errors from Single-Ion Tracks in Integrated Cir‐ cuits," IEEE Transactions on Nuclear Science, **vol.NS-36, no.6,** December 1989.

[9] T. Mnatsakanov, I. **Rostovtsev,** and N. **Philatov, "Investiga‐ tion** of the Effect of Nonlinear Physical Phenomena on Charge Carrier Transport in Semiconductor Devices," Solid-State Elec‐ tronics, **vol.30,** no.6, **pp.579-585,** 1987.

[10] O. **Roos,** "A Note on Photocurrents **in** Extrinsic Semiconduc‐ tors," Solid-State Electronics, **vol.22, pp.229-232,** 1979.

[11] L. **Edmonds,** "Theoretical Prediction of the Impact of Auger

Recombination on Charge Collection from an Ion **Track,"** IEEE
Transactions on Nuclear Science, **vol.38, no.5,** pp.999-1004,
October 1991.

[12] L. Edmonds, "A Simple Estimate **of** Funneling-Assisted Charge
Collection,"l IEEE Transactions on Nuclear Science, VO1.38, **no.2,**
pp.828-833, April 1991.

APPENDIX
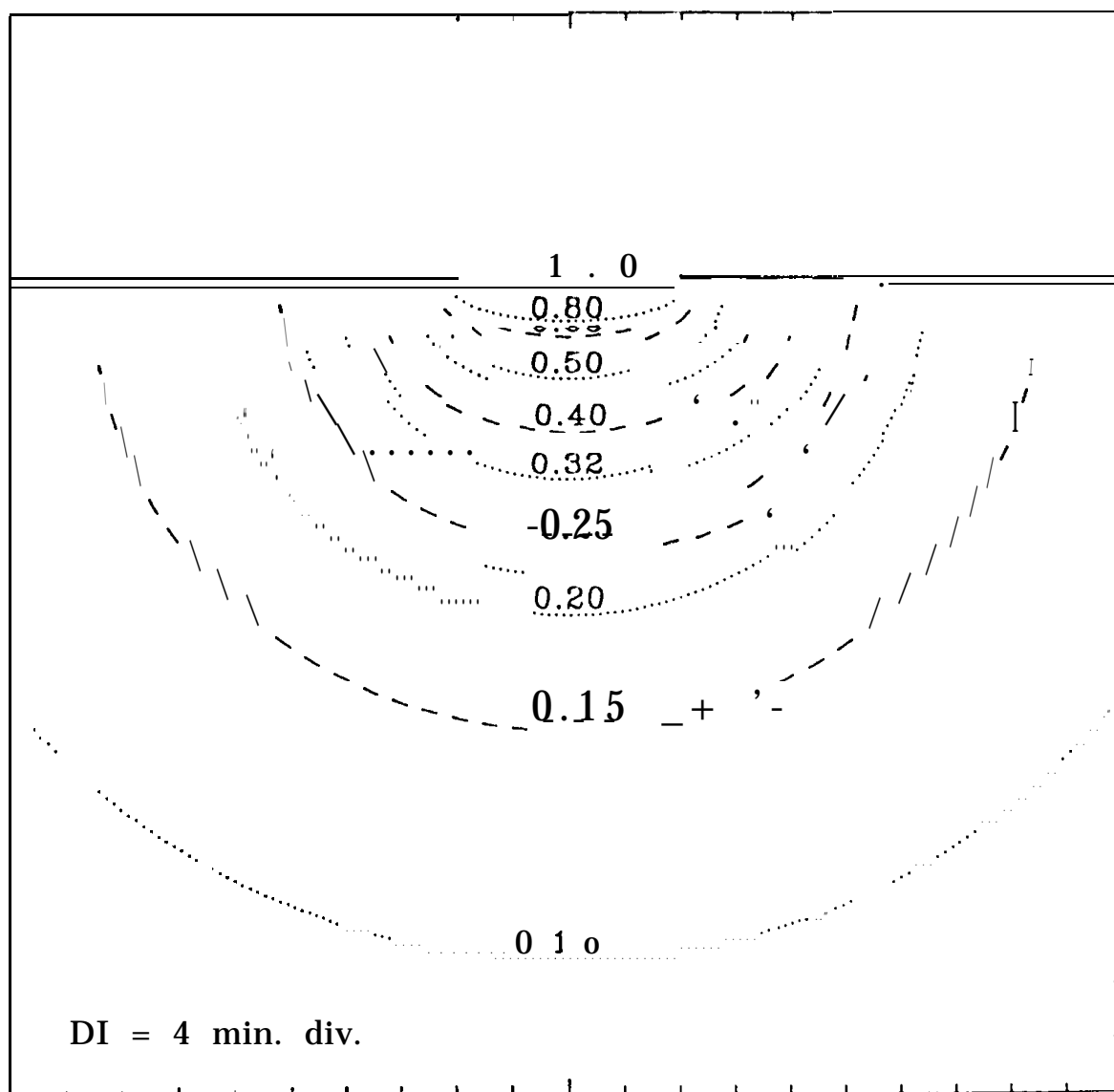
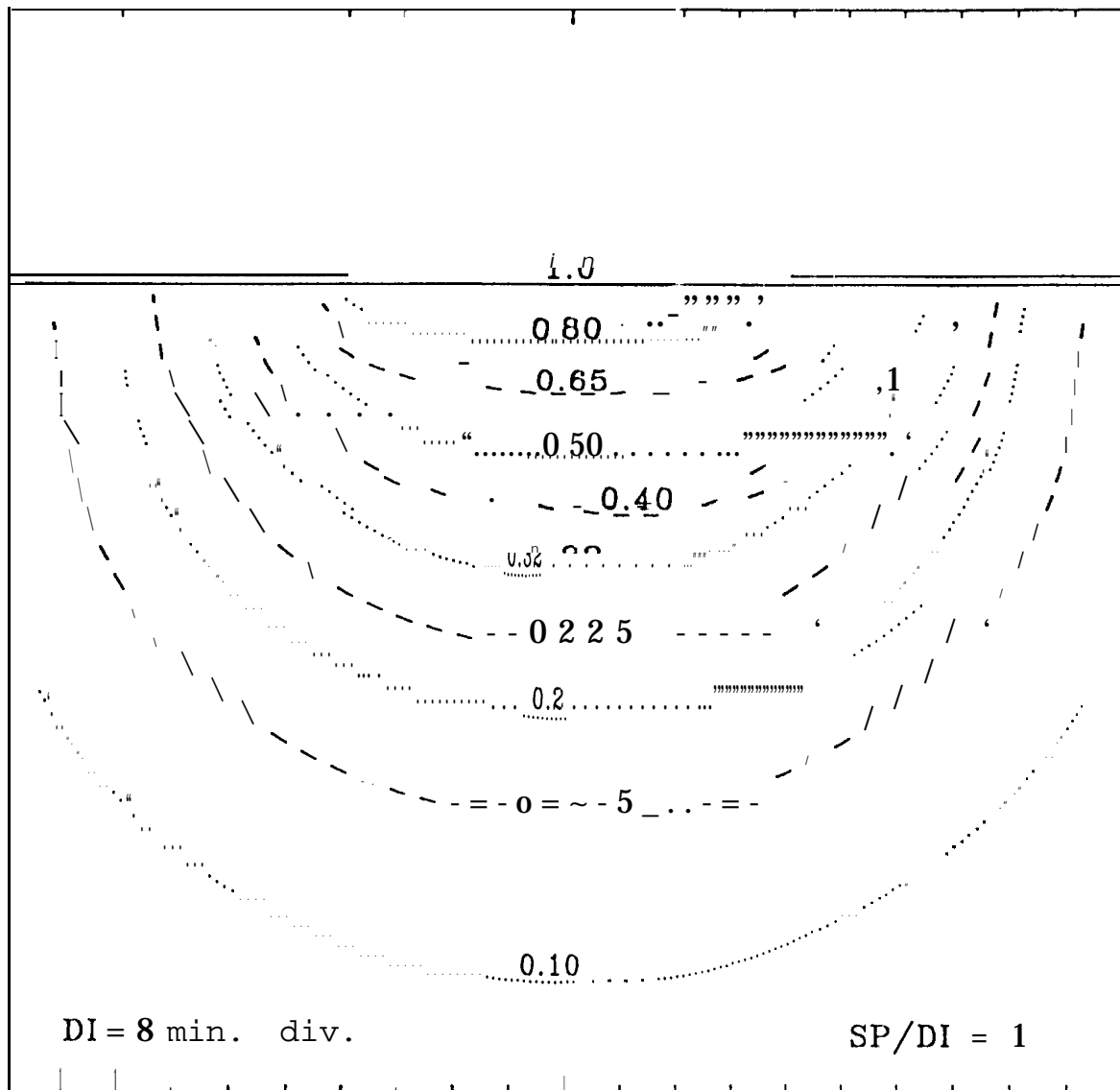Figure Al: An isolated disk. The sink S_1 is at infinity.

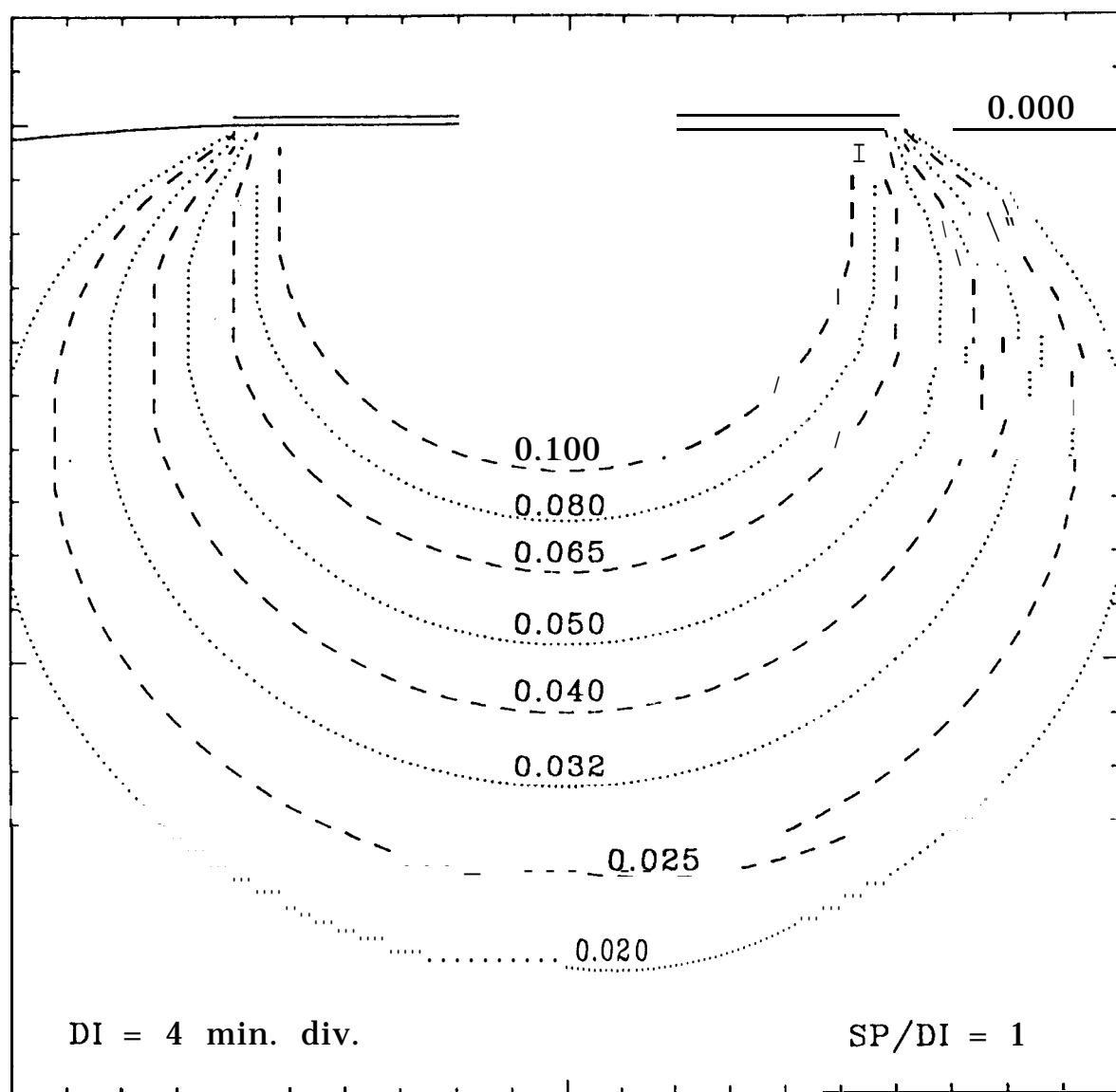Figure A2a: Disk with diameter **DI** surrounded by a sink with lateral separation SP=DI. First of two views.

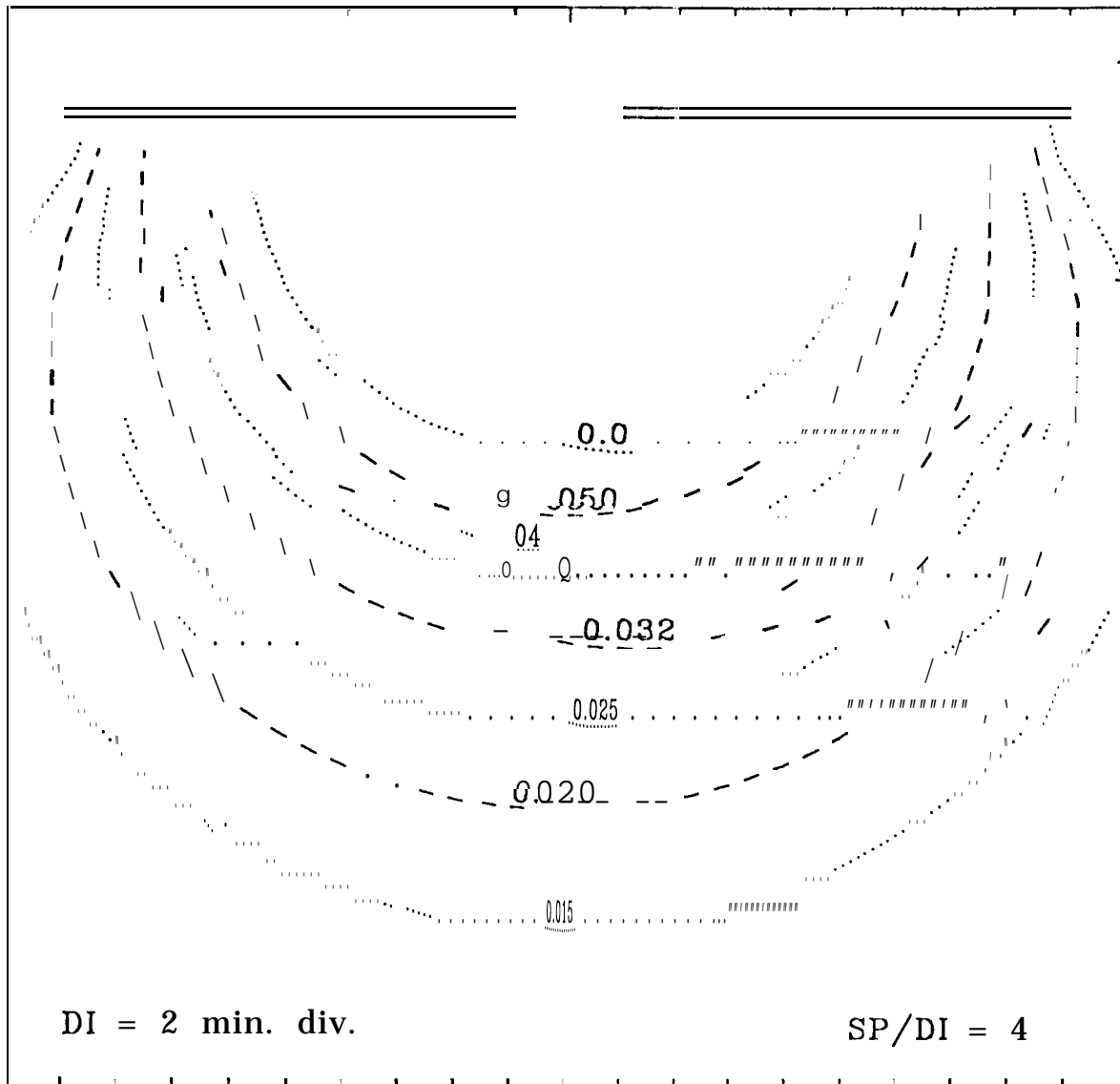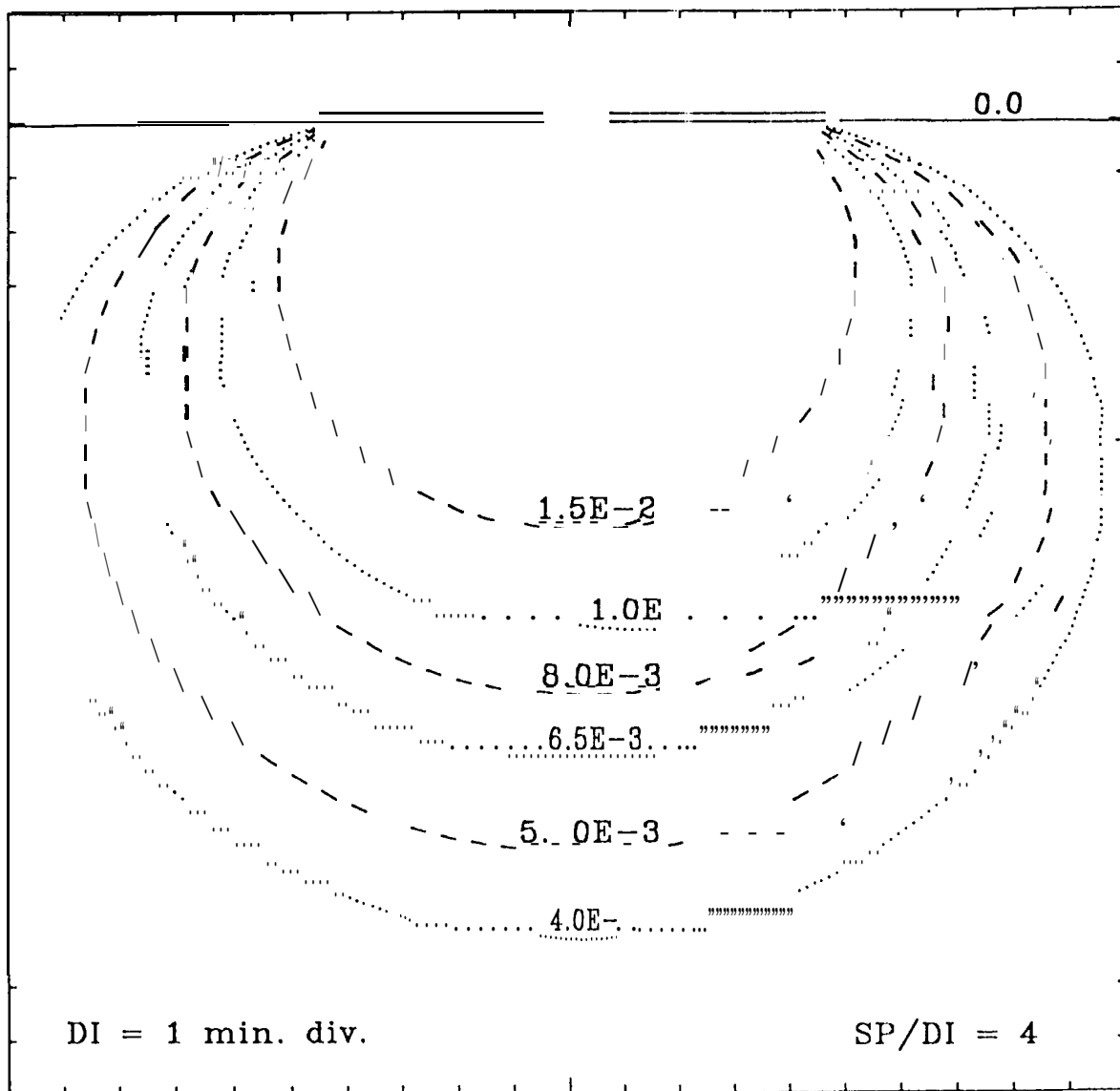Figure A2b: Disk with diameter DI surrounded by a sink with lateral separation SP=DI. Second of two views.
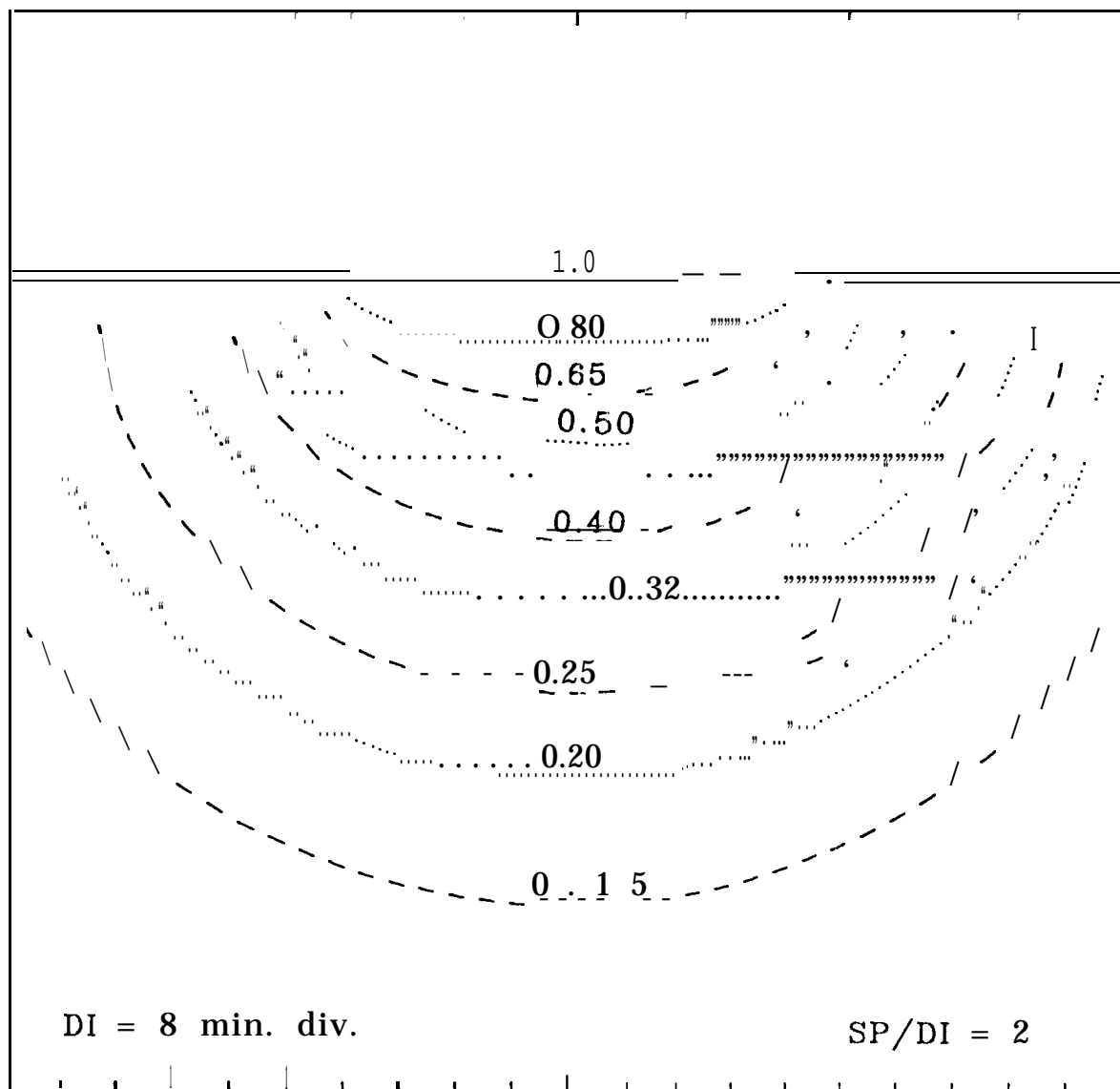
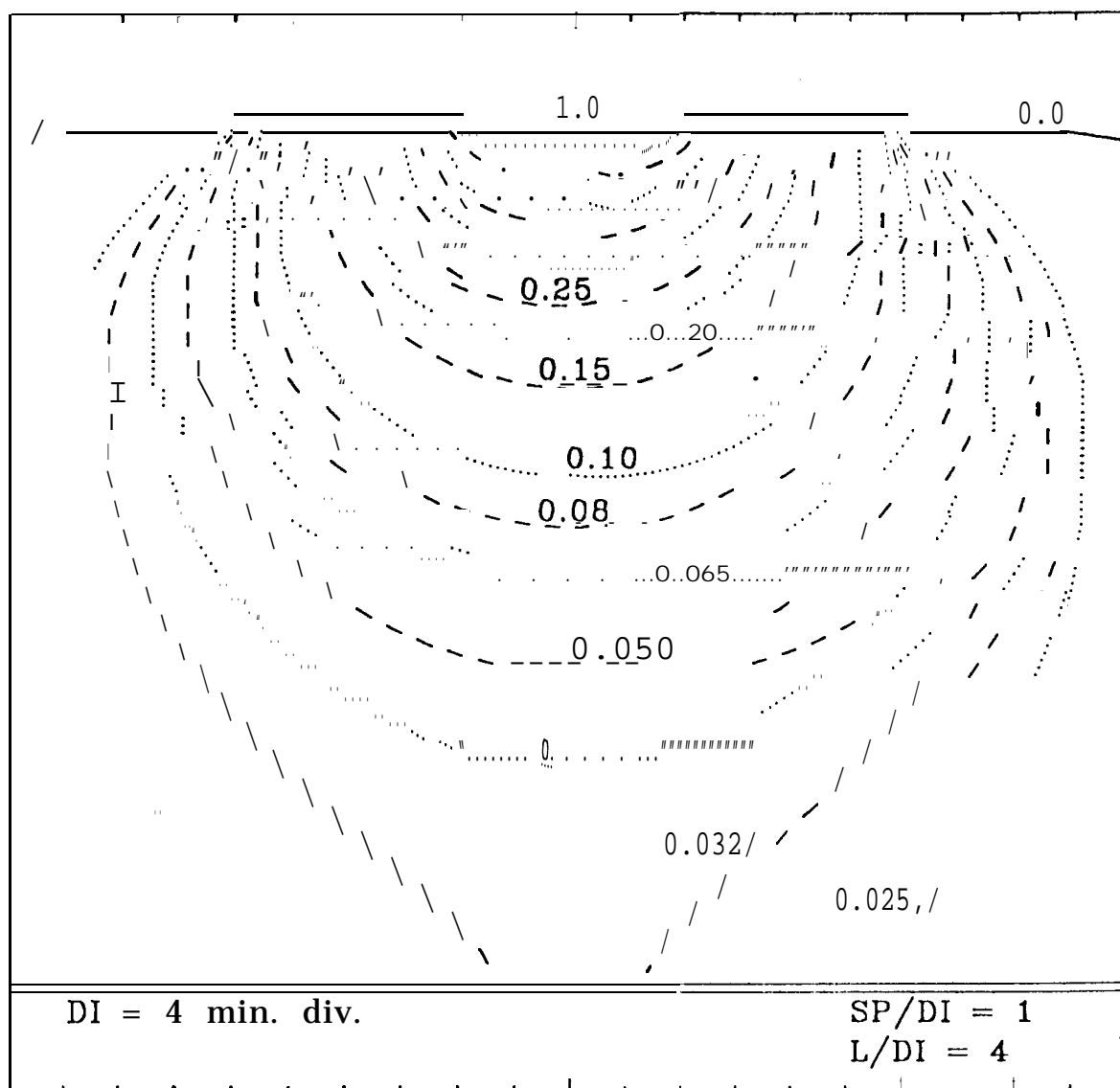Figure A3a: Disk with diameter DI surrounded by a sink with lateral separation SP=2DI. First of three views.

0.150

0.100

0.080

0.065

0.050

0.040

0.032

DI = 4 min. div.

SP/DI = 2
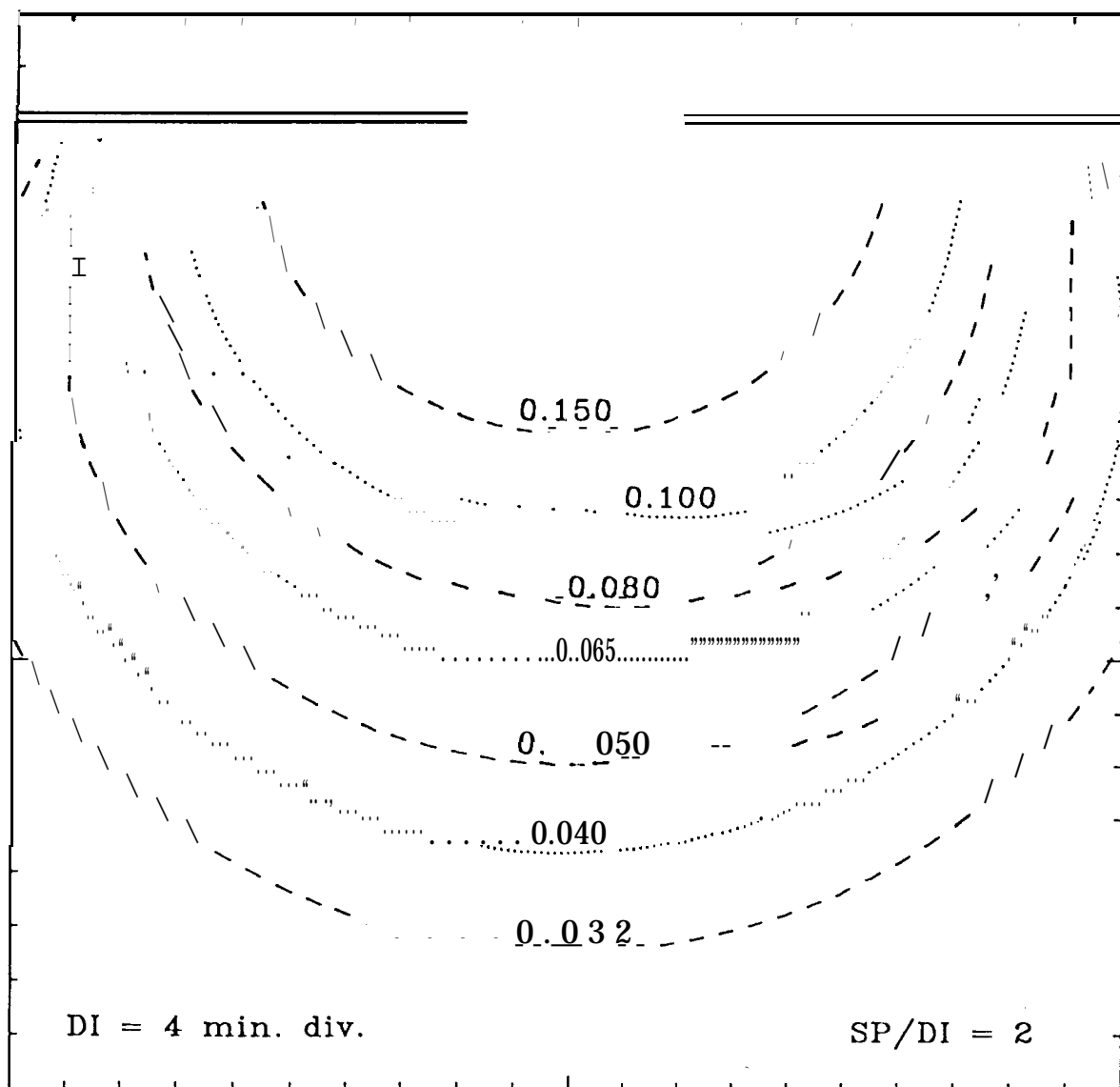
Figure A3b: Disk with diameter DI surrounded by a sink with lateral separation SP=2DI. Second of three views.
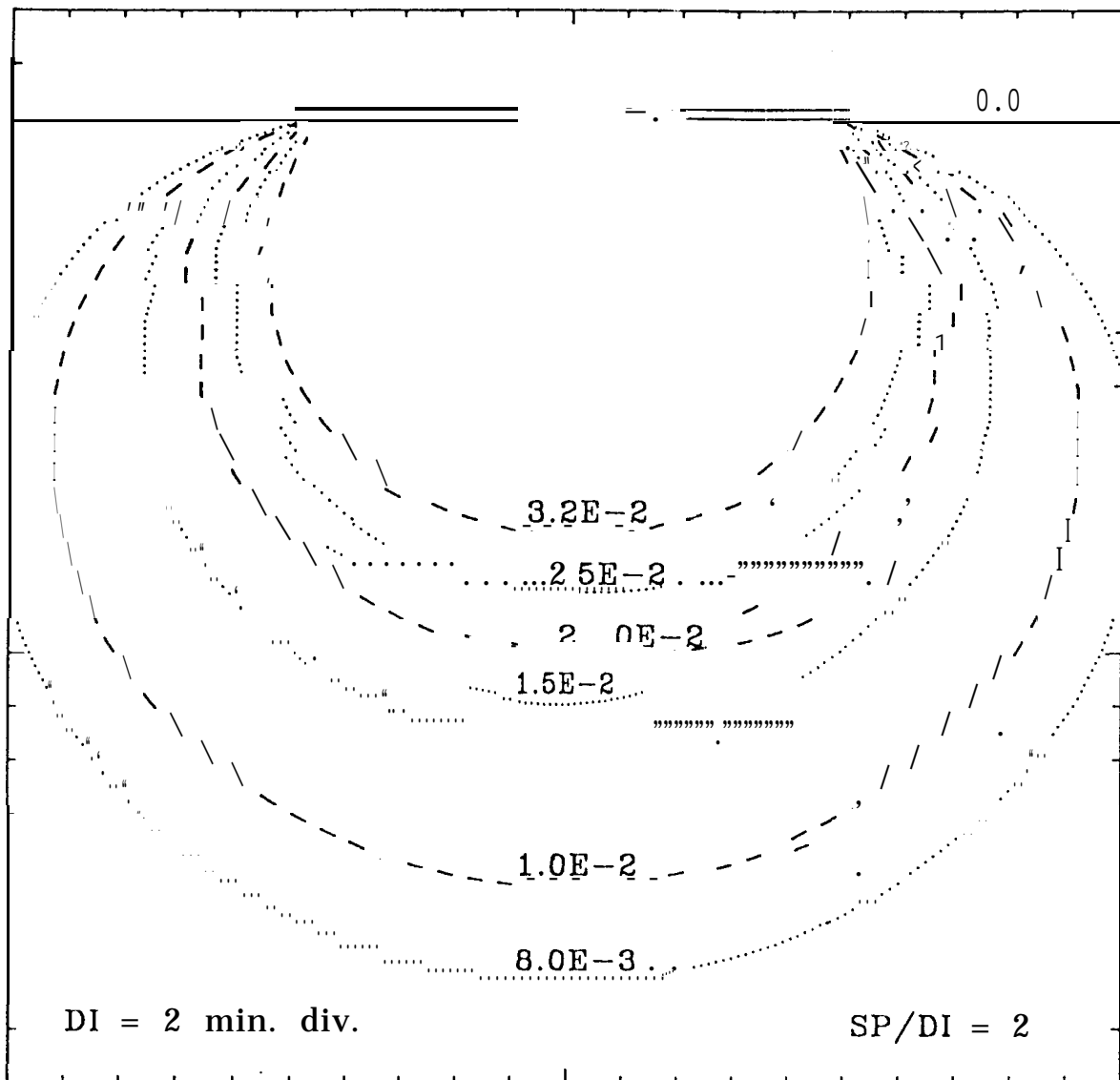
Figure A3c: Disk with diameter **DI** surrounded by a sink with **lateral separation** SP=2DI. Third of three views.
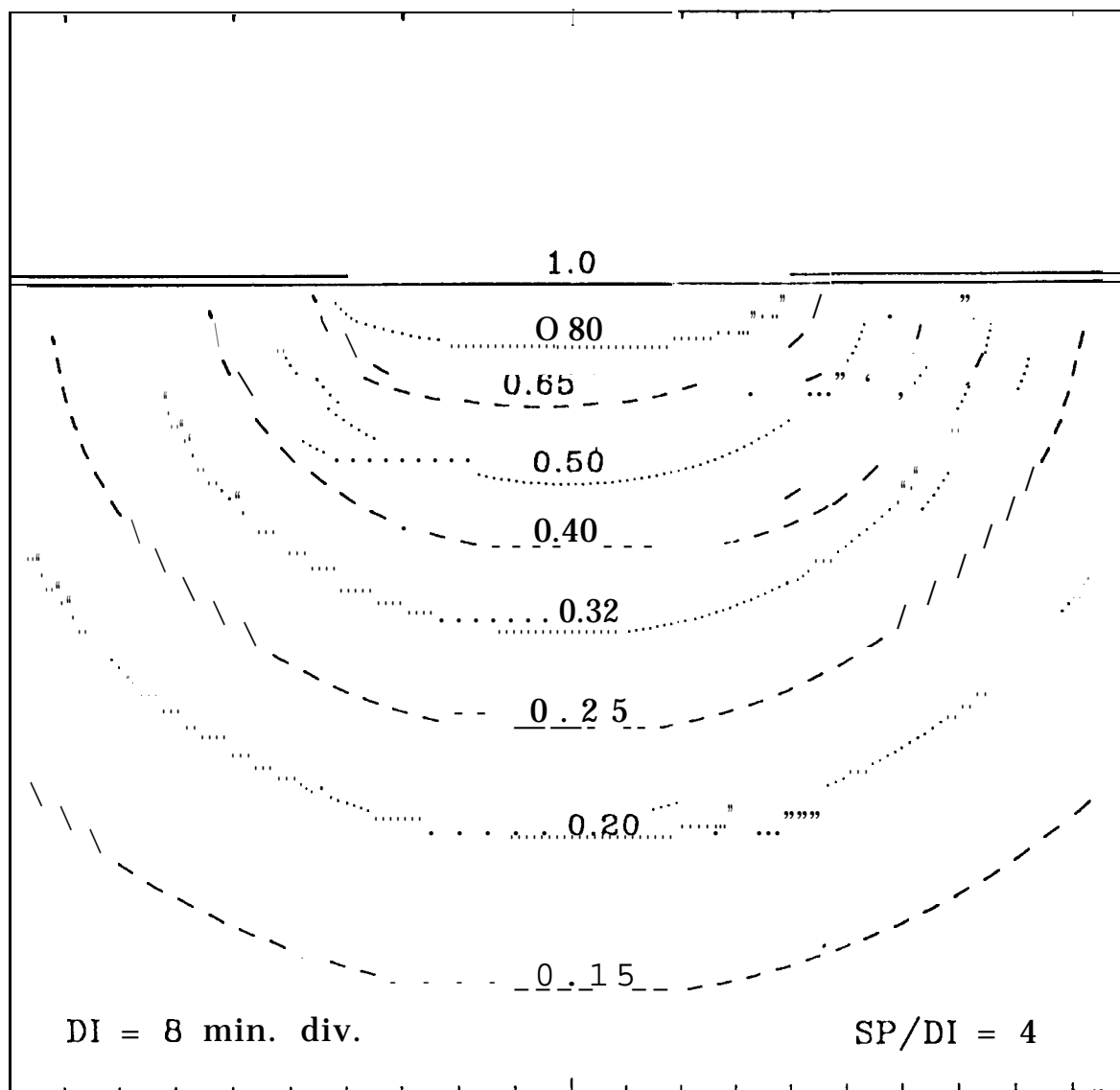
Figure A4a: Disk with diameter **DI** surrounded by a sink with lateral separation **SP=4DI.** First of four views.
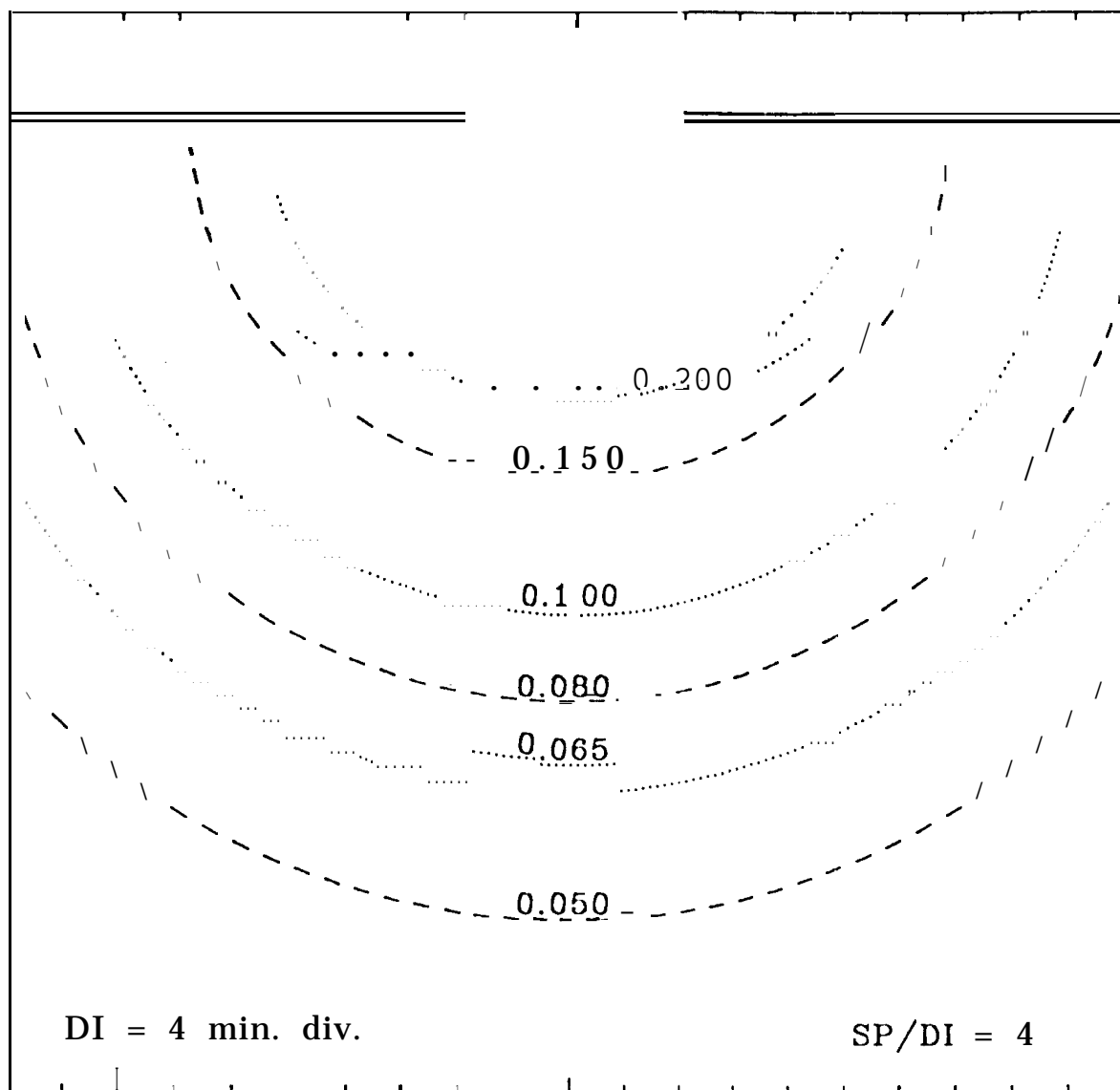
Figure A4b: Disk with diameter DI surrounded by a sink with lateral separation SP=4DI. Second of four views.

Figure A4c: Disk with diameter DI surrounded by a sink with lateral separation SP=4DI. Third of four views.

Figure A4d: Disk with diameter **DI** surrounded by a sink with lateral separation **SP=4DI.** Fourth of four views.
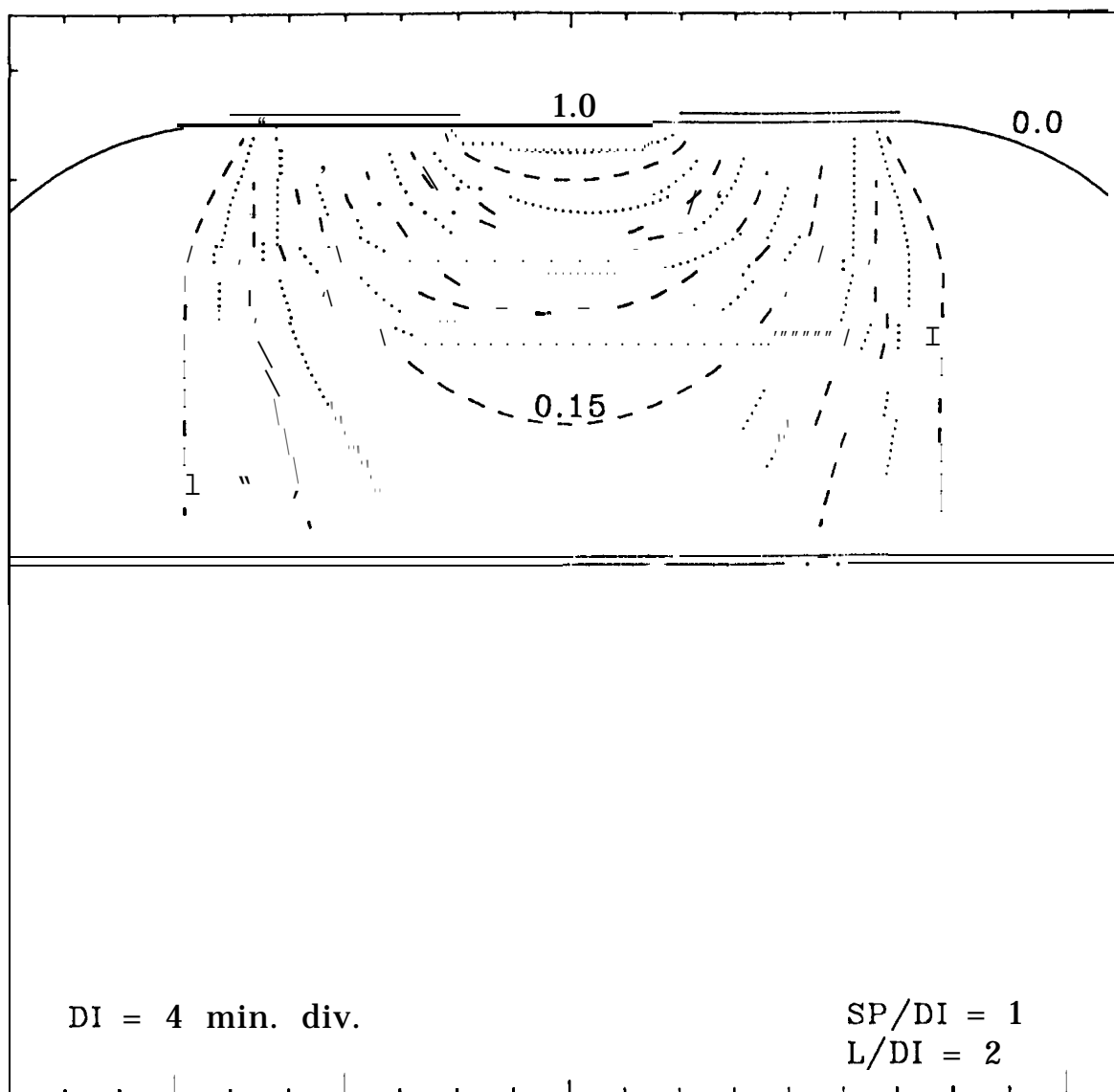
Figure A5 : Disk with diameter DI surrounded by a sink with lateral separation **SP=DI,** and at a distance L=4DI above a reflective plane. Unlabeled contours have the values 0.8, 0.65, 0.5, 0.4, and 0.32.
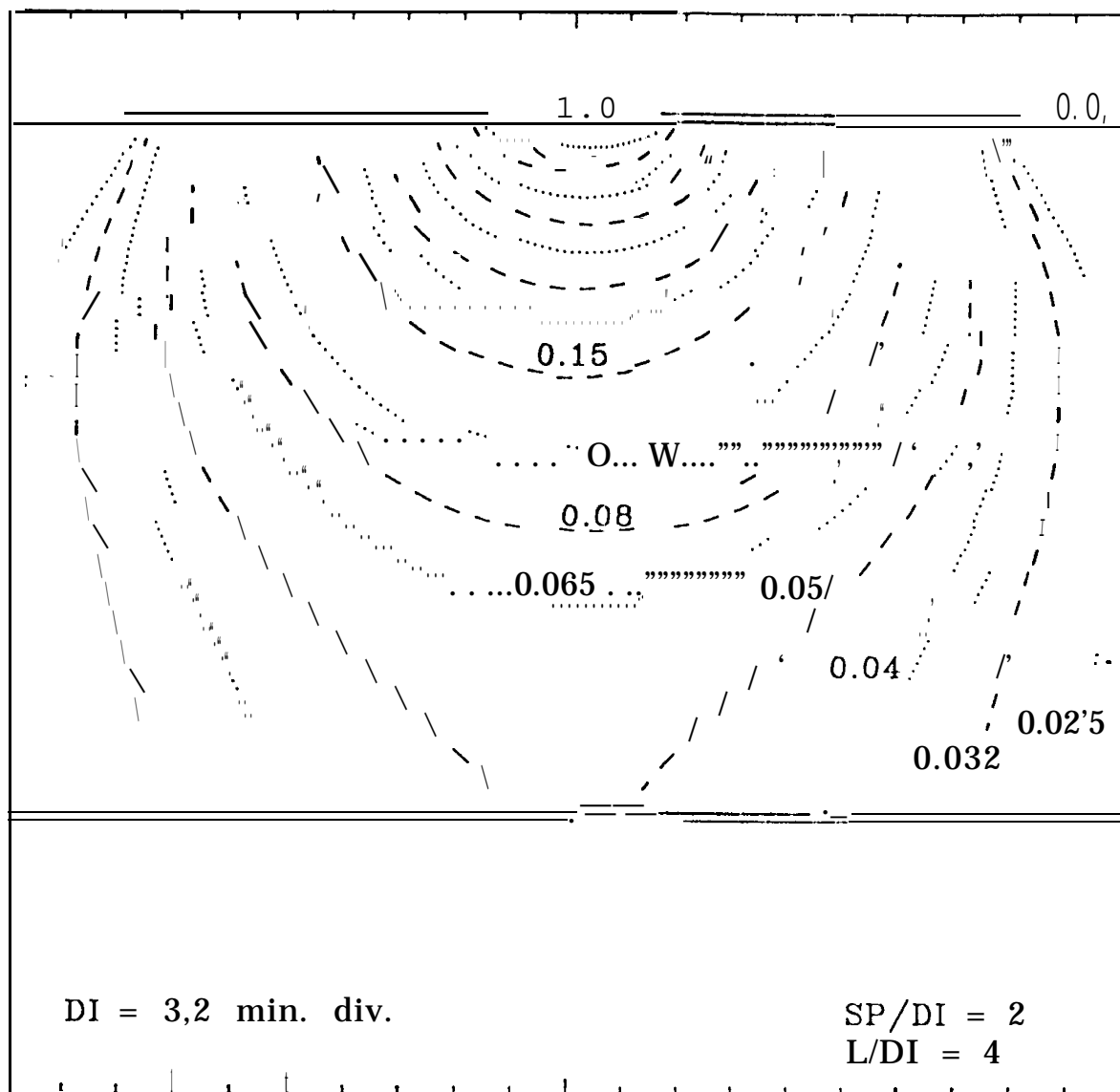
Figure A6 : Disk with diameter **DI** surrounded by a sink with
lateral separation SP=2DI, and at a distance L=4DI above a re-
flective plane. Unlabeled contours have the values 0.8, 0.65,
0.5, 0.4, **0.32, 0.25, and 0.2.**

Figure A7 :   Disk with diameter DI surrounded by a sink with lateral separation SP=DI, and at a distance L=2DI above a reflective plane. The sequence of contour values between 1 and O is 0.8, 0.65, 0.5, 0.4, 0.32, 0.25, 0.2, 0.15, 0.1, 0.08, 0.065, and 0.05.
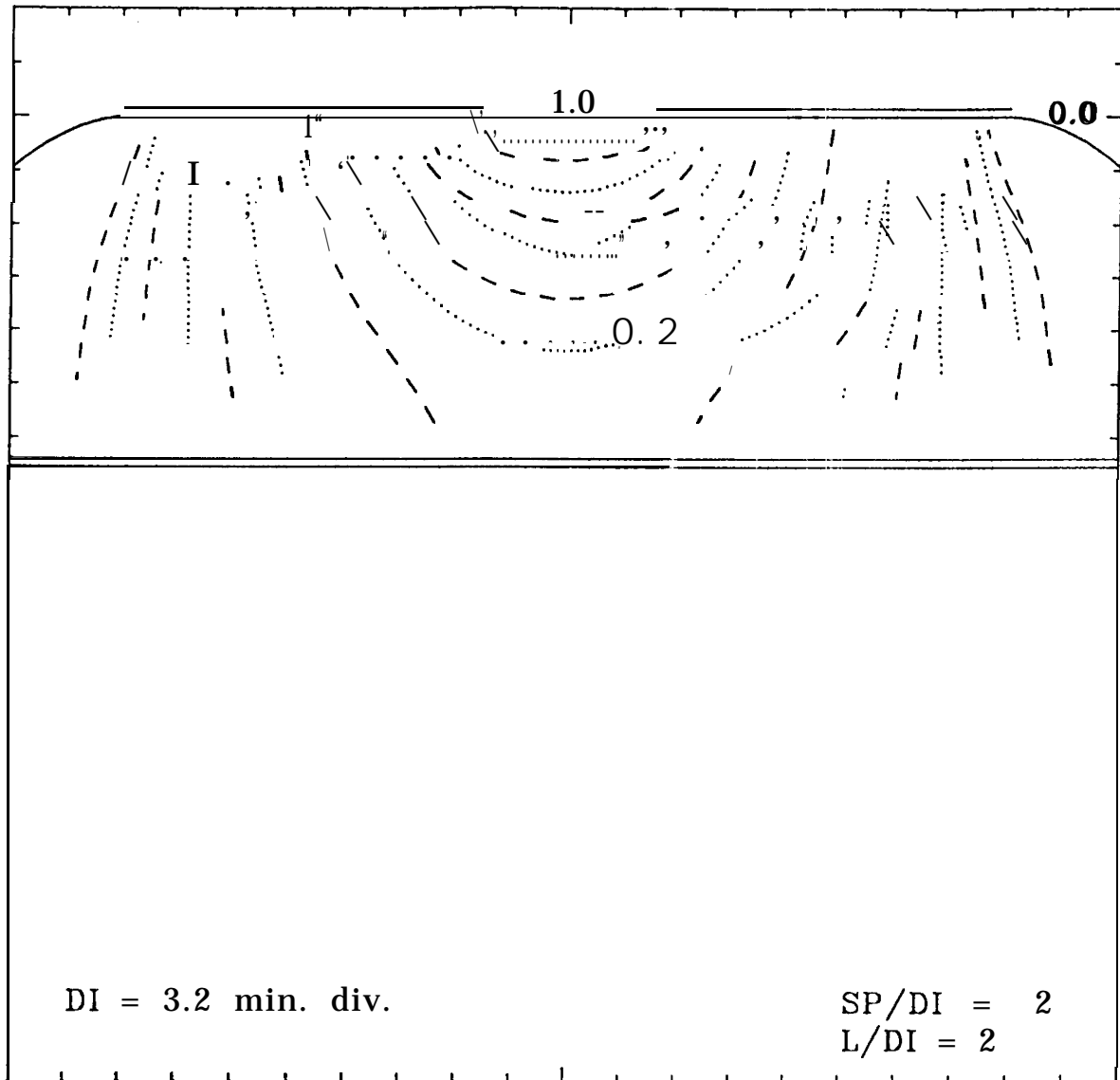
Figure A8 :   Disk with diameter **DI** surrounded by a sink with lateral separation SP=2DI, and at a distance **L=2DI** above a re- flective plane. The sequence of contour values between 1 and O is 0.8, 0.65, 0.5, 0.4, 0.32, 0.25, 0.2, 0.15, 0.1, 0.08, 0.065, 0.05, 0.04, and 0.032.
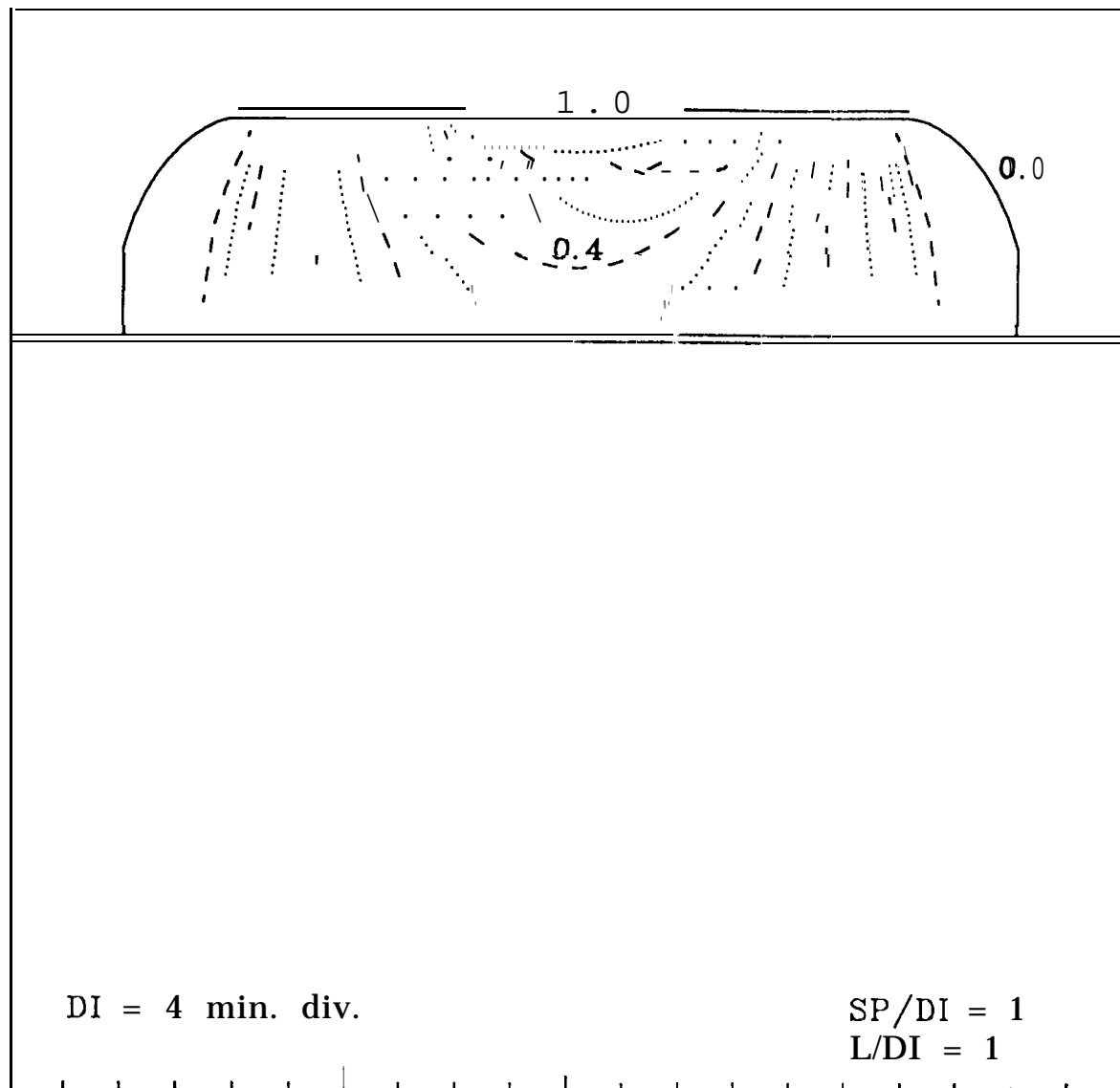
Figure A9: Disk with diameter DI surrounded by a sink with lateral separation SP=DI, and at a distance L=DI above a reflective plane. The sequence of contour values between 1 and O is 0.8, 0.65, 0.5, 0.4, 0.32, 0.25, 0.2, 0.15, 0.1, 0.08, 0.065, and 0.05.
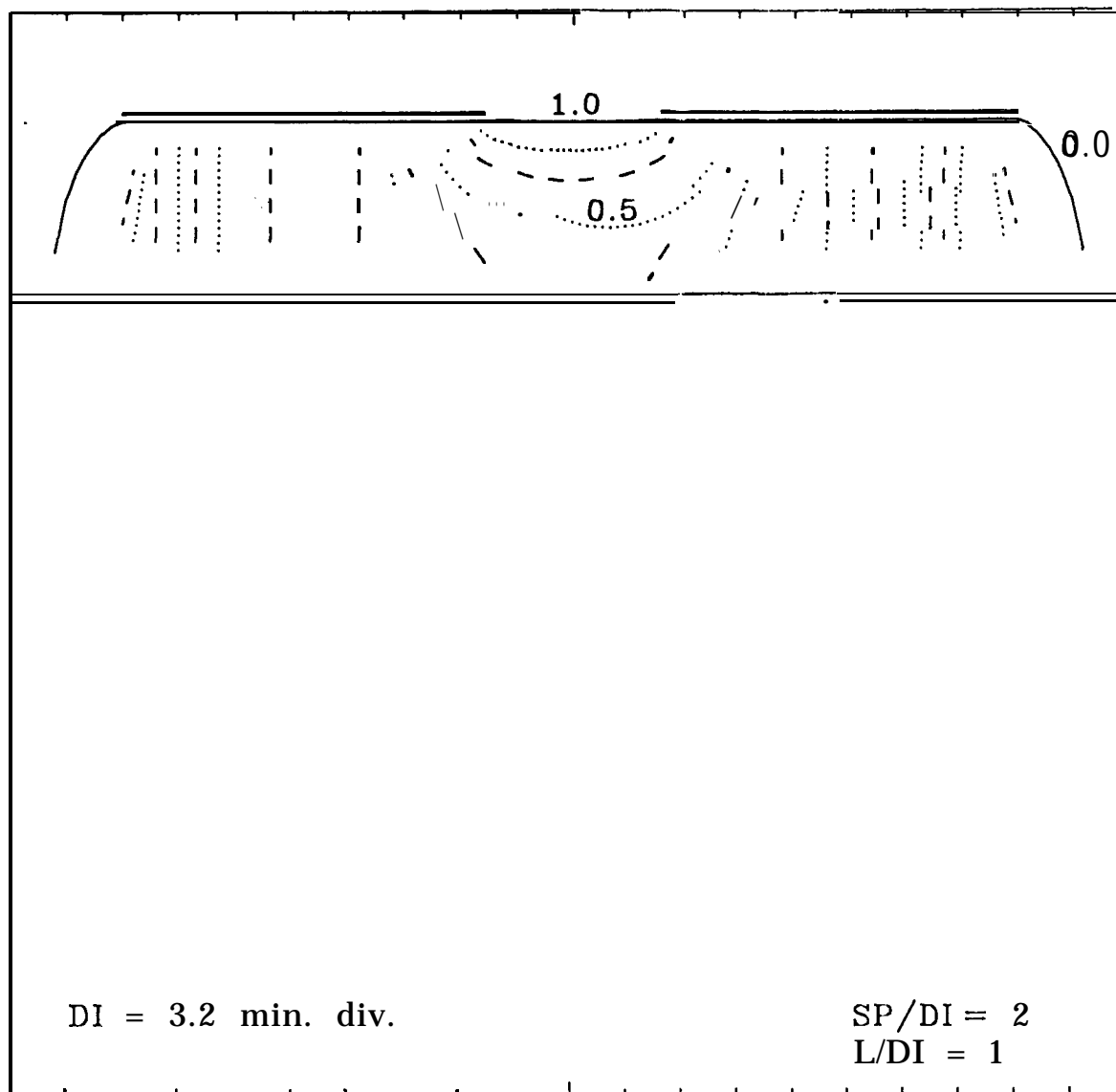
Figure A1O: Disk with diameter DI surrounded by a sink with lateral separation SP=2DI, and at a distance L=DI above a reflective plane. The sequence of contour values between 1 and O is 0.8, 0.65, 0.5, 0.4, 0.32, 0.25, 0.2, 0.15, 0.1, 0.08, 0.065, 0.05, 0.04, and 0.032.